The role of sediment subduction and crustal growth in Hercynian plutonism: isotopic and trace element evidence from the Sardinia

JOURNAL OF PETROLOGY | VOLUME 36 | NUMBER 5 | PAGES 1305–1332 | 1995

SIMONE TOMMASINI[1,2,*], GIAMPIERO POLI[1] AND ALEX N. HALLIDAY[2]
[1]DIPARTIMENTO DI SCIENZE DELLA TERRA, PIAZZA UNIVERSITÀ, 06100 PERUGIA, ITALY
[2]DEPARTMENT OF GEOLOGICAL SCIENCES, UNIVERSITY OF MICHIGAN, 1006 C. C. LITTLE BUILDING, ANN ARBOR, MI 48109-1063, USA

The Role of Sediment Subduction and Crustal Growth in Hercynian Plutonism: Isotopic and Trace Element Evidence from the Sardinia–Corsica Batholith

The calc-alkaline association of the Hercynian Sardinia–Corsica Batholith consists of multiple coalescent granitoid plutons and minor gabbroic complexes. Isotopic and trace element data are presented for selected gabbros and I-type granitoids representative of the parental mantle- and crust-derived magmas, respectively. The gabbros belong to normal calc-alkaline suites and have marked relative enrichments in Rb, Ba, K and Pb in primitive mantle-normalized trace element diagrams. The granitoids belong to high-K calc-alkaline suites and have fairly uniform trace element compositions resembling volcanic arc granitoids (VAG). A significant overlap in Sr and Nd isotope compositions is observed between gabbros and granitoids.

Geochemical and isotopic data provide evidence for the origin of the gabbros from mantle sources enriched in incompatible trace elements through recycling of sediments via subduction zones, whereas the granitoids were derived from crustal sources composed mainly of igneous protoliths with relatively homogeneous composition. Sr and Nd isotope compositions of gabbros and granitoids are consistent with both the mantle enrichment process and the formation of the igneous crustal sources occurring at ~450 Ma, during the earlier calc-alkaline igneous activity.

The connection between Hercynian and Ordovician igneous activity has important and new implications for the Palaeozoic evolution of the Sardinia and Corsica lithosphere, and permits the Hercynian orogeny to be placed in a wider geodynamic setting, consisting of three main phases. The Ordovician pre-collisional phase was characterized by a N–NE-dipping subduction of an oceanic plate under a continental plate with emplacement of acid and subordinate basic–intermediate volcanic and intrusive rocks. The subcontinental mantle underneath Sardinia and Corsica experienced enrichment in incompatible trace elements through recycling of sediments. Major crustal accretion also occurred with underplating of basaltic magmas. The Devonian collisional phase was characterized by the collision of two continental plates after the total consumption of the oceanic plate. Crustal thickening processes took place together with regional metamorphic events that recorded a clockwise P–T–t *path. The Carboniferous post-collisional phase was characterized by isostatic and thermal readjustments following crustal thickening that caused extensive partial melting. Large quantities of I-type granitoids and subordinate gabbroic complexes were emplaced in the middle–upper crust and formed the main frame of the Sardinia–Corsica Batholith.*

This geodynamic model is consistent with the Palaeozoic evolution of other sectors of Western Europe suggested on the basis of geological, geochronological and palaeomagnetic data. The palaeomagnetic restoration of the Late Palaeozoic position of Sardinia and Corsica close to Southern France suggests that Sardinia and Corsica could have been portions of the southern edge of the Armorican plate that, during Siluro-Devonian, collided with the Ibero-Aquitanian plate after the total consumption of the Late Cambro-Ordovician South Armorican and/or Massif Central Ocean.

KEY WORDS: *crustal growth; Hercynian orogeny; mantle enrichment; radiogenic isotopes; Sardinia–Corsica Batholith*

INTRODUCTION

The Sardinia–Corsica Batholith (SCB) formed as a result of continental collision (e.g. Carmignani *et al.*, 1992) and is largely composed of crust-derived granitoids and subordinate mantle-derived gabbroic

*Corresponding author. Present address: Dipartimento di Scienza del Suolo e Nutrizione della Pianta, Piazzale Delle Cascine 16, 50144 Firenze, Italy

complexes (Bralia *et al.*, 1982; Cocherie, 1984; Poli *et al.*, 1989; Rossi & Cocherie, 1991; Cocherie *et al.* 1994) (Fig. 1). The interactions between crust- and mantle-derived magmas resulted in a wide variety of hybrid magmas ranging from homogeneous, completely blended, tonalitic intrusions to heterogeneous, mechanically mixed, mafic enclave-bearing granitoids (Poli *et al.*, 1989; Rossi & Cocherie, 1991; Zorpi *et al.*, 1991; Tommasini, 1993). As such, isotopic and geochemical characteristics of these hybrid magmas cannot serve as unique indicators to assess the timing of crustal growth and the nature of source reservoirs during the Hercynian orogeny in Sardinia and Corsica.

In this paper we discuss geochemical and isotopic compositions of samples, representative of parental crust- and mantle-derived magmas, selected from >200 calc-alkaline I-type granitoids and coeval gabbroic complexes from the SCB (Tommasini, 1993). The calc-alkaline association makes up most of the Batholith (Fig. 1). Isotopic and trace element compositions of parental magmas permit the assessment of the geochemical characteristics of source reservoirs and the relative role of crustal recycling and new mantle additions to the continental crust. Inferences on the geodynamic setting in this sector of the European Hercynian Belt are also discussed, along with a comparison with models for the Palaeozoic evolution of Western Europe.

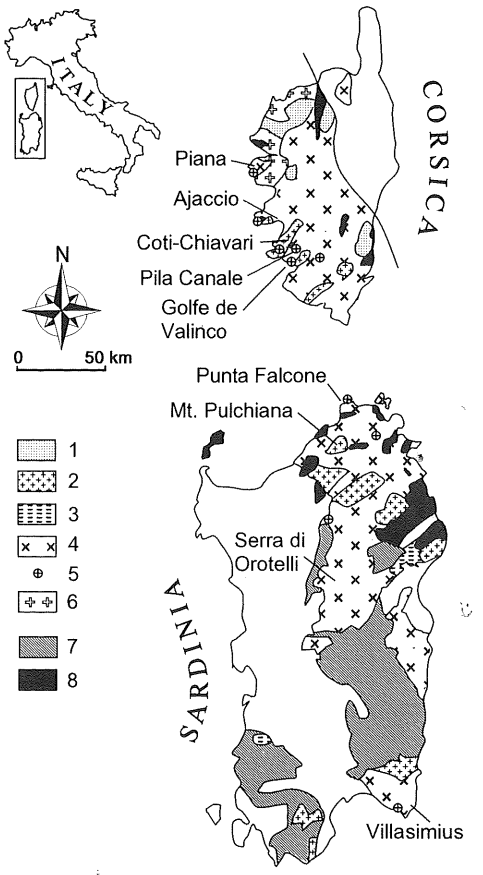

Fig. 1. Schematic geological map of the Sardinia–Corsica Batholith showing outcropping areas of the main metamorphic and igneous rocks. 1, Permian A-type volcanics and subvolcanics; Hercynian Orogeny: 2, post-tectonic leucogranites; 3, late-tectonic peraluminous granitoids; 4, late-tectonic metaluminous granitoids; 5, main gabbroic complexes; 6, Mg–K granitoids; 7, low-grade metamorphic rocks; 8, medium- to high-grade metamorphic rocks. 2, 4 and 5 form the calc-alkaline association; 6 forms the Mg–K or shoshonitic association. Sampling locations along the north–south transverse of the Batholith are reported.

GEOLOGICAL BACKGROUND

Sardinia and Corsica are two islands located in the Mediterranean Sea, west of Italy. Their basement consists of metamorphic terrains, multiple coalescent granitoid plutons and subordinate gabbroic complexes (Fig. 1). The main metamorphic and magmatic features of the two islands were formed as a result of the Hercynian orogeny, related to continent–continent collision (e.g. Rossi & Cocherie, 1991; Carmignani *et al.*, 1992).

The metamorphic grade of the pre-Hercynian basement rocks progressively increases towards the NE from greenschist facies in Southern and Central Sardinia, to amphibolite facies with migmatites in Northern Sardinia and Corsica (Fig.1). Franceschelli *et al.* (1989) recognized two main metamorphic events in the amphibolite facies rocks of Northern Sardinia (Table 1). The first metamorphic event occurred at ~350 Ma and was characterized by medium-pressure (7–8 kbar) and high-temperature (700–800°C) conditions. The second, low-pressure and medium-temperature (2–3 kbar, 600°C) metamorphic event occurred at ~300 Ma. The two metamorphic events define a clockwise P–T–t path typical of homogeneously thickened orogenic belts. An earlier metamorphic event (~13–17 kbar, Libourel & Vielzeuf, 1988; Ménot & Orsini, 1990) probably took place before the medium-pressure–high-temperature metamorphism and caused the development of high-pressure granulite–eclogite parageneses that occur as relics in some amphibolite facies rocks of Northern Sardinia and Corsica (Miller *et al.*, 1976; Ghezzo *et al.*, 1979; Palagi *et al.*, 1985).

The Hercynian igneous activity (350–280 Ma, Table 1) involved large volumes of crust-derived granitoids and minor mantle-derived gabbroic complexes (<5%) that were emplaced into the upper–middle crust and formed the SCB (e.g. Bralia *et al.*, 1982; Poli *et al.*, 1989; Rossi & Cocherie, 1991; Tommasini, 1993; Cocherie *et al.*, 1994). The emplacement of plutons was followed by calc-alka-

Table 1: Radiometric dating and palaeontological data for the main Palaeozoic events recorded in the rocks of Sardinia and Corsica

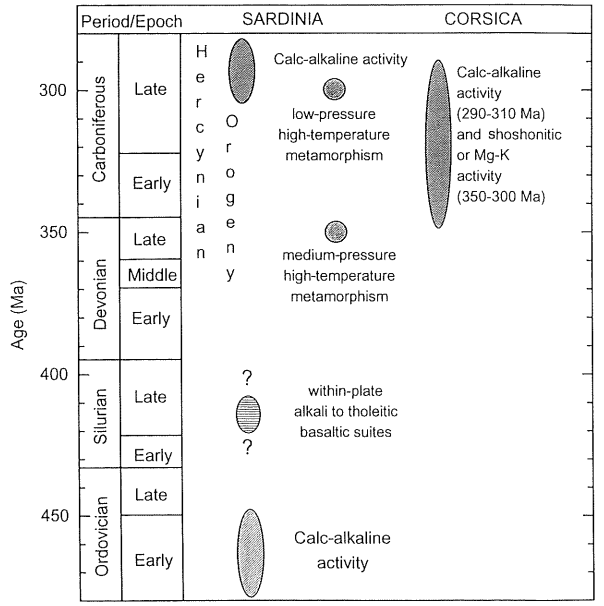

Data sources: Beccaluva *et al.* (1985); Franceschelli *et al.* (1989); Ménot & Orsini (1990); Rossi & Cocherie (1991); Cocherie *et al.* (1994). The age of Silurian basalts is on the basis of palaeontological data from Memmi *et al.* (1983) and Carmignani *et al.* (1986).

line volcanism in the Permian with eruption of intermediate and acid lava flows and ignimbrites (e.g. Vellutini, 1977).

Two earlier periods of igneous activity occurred in the Ordovician and Silurian (Table 1). Palaeontological data and radiometric dating indicate that in Sardinia the former igneous activity occurred between Arenigian and Caradocian (e.g. Beccaluva *et al.*, 1985; Carmignani *et al.*, 1986). This igneous activity consists of acid plutonic rocks (at present orthogneisses) and basic to acid volcanic rocks (at present metabasalts, metandesites and metarhyolites). Metavolcanic rocks mainly outcrop along a NNW–SSE belt from Nurra, North-Western Sardinia, to Sarrabus, South-Eastern Sardinia, whereas metaplutonic rocks outcrop in Gallura, North-Eastern Sardinia (Carmignani *et al.*, 1986). On the basis of geochemical diagrams to discriminate among different magma series in metaigneous rocks (e.g. Nb/Y, Winchester & Floyd, 1977), Memmi *et al.* (1983) established that the entire suite has a calc-alkaline affinity and can be related to active continental margin settings. Orthogneisses outcropping in the basement of Corsica were also referred to a Lower Palaeozoic igneous activity (Vezat, 1986; Ménot & Orsini, 1990) on the basis of analogies with those of Northern Sardinia dated at ~450 Ma (Beccaluva *et al.*, 1985). No radiometric dating is, however, available to support an Ordovician igneous activity in Corsica.

The Silurian igneous activity consists of alkali to tholeiitic basaltic suites (at present metabasalts and metagabbros). In Sardinia, they outcrop within well-characterized Upper Ordovician–Devonian sequences of fossiliferous metasediments in greenschist facies (e.g. Carmignani *et al.*, 1986). On the basis of their geochemical characteristics (e.g. Zr–Ti–Y, Pearce & Cann, 1973), Memmi *et al.* (1983) established that the Silurian basic rocks have a within-plate affinity and suggested a continental rift environment for this episode of igneous activity. In Corsica, remnants of within-plate basaltic suites have been correlated with the Silurian basic rocks of Sardinia (Ricci & Sabatini, 1978).

These Lower Palaeozoic igneous rocks outcrop within pre-Carboniferous metasedimentary sequences and have been affected by the Barrovian-type metamorphism of the Hercynian orogeny.

Finally, subvolcanic and volcanic alkaline rocks, forming ring complexes, were emplaced in Corsica during the Permian (Fig.1). They consist of A-type acid magmas related to a within-plate anorogenic setting (Bonin, 1980, 1988).

The Sardinia–Corsica Batholith

The granitoid plutons of the SCB outcrop over some 12 000 km^2 (Fig. 1). Intrusive rocks were emplaced during the post-collisional phase of the Hercynian orogeny in forced (syn- to late-tectonic intrusions) and permissive (post-tectonic intrusions) regimes. Calc-alkaline and shoshonitic intrusive associations have been recognized (e.g. Ménot & Orsini, 1990; Cocherie *et al.*, 1994). The calc-alkaline association makes up most of the Batholith (Table 2) and was emplaced from 310 to 280 Ma, whereas the Mg–K shoshonitic association (e.g. Orsini, 1980; Ménot & Orsini, 1990; Cocherie *et al.*, 1994), outcrops in minor amount in North-Western Corsica and was emplaced from 350 to 300 Ma (Table 1).

The composition of the calc-alkaline late-tectonic intrusions ranges from gabbro and diorite to tonalite, granodiorite, monzogranite and leucogranite, whereas that of post-tectonic intrusions is restricted to leucogranite (Fig. 2). The shoshonitic association exhibits a compositional range from monzogabbros and monzodiorite to monzonite, monzogranite and leucogranite (Table 2). Basic rocks occur as stratified gabbroic complexes and undifferentiated septa enclosed in the granitoids, and as ubiquitous mafic microgranular enclaves thoroughly dispersed within granitoid plutons except the post-tectonic leucogranites. The abundance of mafic microgranular enclaves decreases from ~10% in the tonalitic

Table 2: Main intrusive rocks of the Sardinia–Corsica Batholith

Lithology	General characteristics	Abundance (outcrop surface %)	Classifications		
			1	2	3
tonalite, granodiorite, monzogranite	peraluminous with restitic enclaves and MME	1–2	syn-tectonic	complex A	
monzonite, monzogranite, leucogranite	metaluminous with MME and coeval gabbroic complexes	5–10			Mg–K or shoshonitic association
tonalite, granodiorite	metaluminous with MME and coeval gabbroic complexes	10–20	late-tectonic	complex C	γ 1 group of the calc-alkaline association
granodiorite, monzogranite	metaluminous with MME and coeval gabbroic complexes	50–60	late-tectonic	complex D	γ 2 group of the calc-alkaline association
granodiorite, granite	peraluminous with restitic enclaves and MME	5	late-tectonic	complex F	
leucogranite	metaluminous	20–25	post-tectonic	complex E	γ 3 group of the calc-alkaline association

MME, mafic microgranular enclaves.
Classifications: 1, Carmignani *et al.* (1986, 1987); Di Vincenzo & Ghezzo (1992). 2, Poli *et al.* (1989). 3, Orsini (1980); Ménot & Orsini (1990).

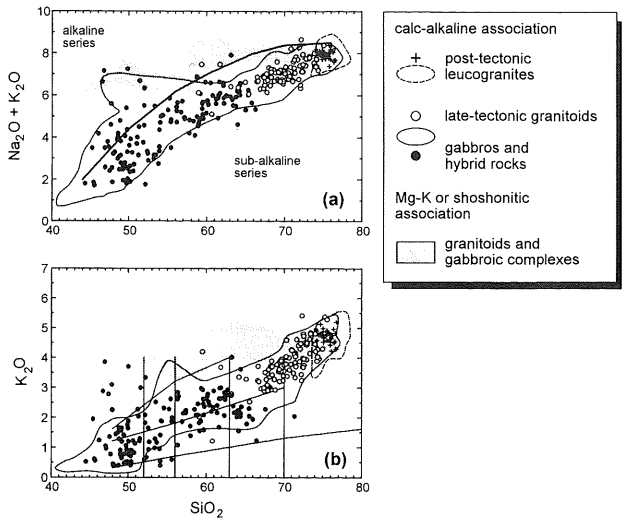

Fig. 2. Alkalis (a) and K_2O (b) vs SiO_2 diagrams of all studied samples (circles and crosses) belonging to the calc-alkaline association of the Sardinia–Corsica Batholith. Fields of the calc-alkaline and shoshonitic association are reported from previous compilations by Orsini (1980), Bralia *et al.* (1982) and Cocherie (1984). Subdivision line between alkaline and sub-alkaline series (a) is from Miyashiro (1978), whereas those between the various calc-alkaline associations (b) are from Peccerillo & Taylor (1976).

plutons to 1–2% in the monzogranitic plutons. Acid plutons (granodiorites, monzogranites, leucogranites) form >70–80% of the Batholith (Table 2), and are mainly metaluminous I-type granitoids, with minor amounts of peraluminous S-type granitoids (Table 2).

GENERAL CHARACTERISTICS OF HERCYNIAN CALC-ALKALINE MAGMAS

Hercynian calc-alkaline suites of Sardinia and Corsica have been extensively studied (e.g. Di Simplicio *et al.*, 1974; Orsini, 1980; Bralia *et al.*, 1982; Cocherie, 1984; Rossi, 1986; Poli *et al.*, 1989; Ménot & Orsini, 1990; Rossi & Cocherie, 1991; Poli & Tommasini, 1991*a*; Tommasini & Poli, 1992; Tommasini, 1993; Cocherie *et al.* 1994), and a considerable database is available to identify their geochemical and petrographic characteristics clearly.

The calc-alkaline association can be distinguished from the shoshonitic association on the basis of major element diagrams (Fig. 2) as well as trace element contents and mineral assemblages (Orsini, 1980; Ménot & Orsini, 1990; Rossi & Cocherie, 1991). The spectrum of calc-alkaline intrusions straddles the normal and high-K calc-alkaline fields, passing from gabbroic to granitoid rocks (Fig. 2b). The post-tectonic leucogranites cluster toward high silica and alkali contents (Fig. 2), and cannot be distinguished from evolved products of the late-tectonic granitoids on a geochemical basis. However, the post-tectonic leucogranites exhibit features such as (1) the absence of mafic microgranular enclaves, (2) a compositional homogeneity at the scale of a single pluton, (3) emplacement in permissive tectonic regimes and (4) emplacement along SW–NE structural directions perpendicular to those of late-tectonic granitoids (e.g. Rossi, 1986; Ménot & Orsini, 1990; Rossi & Cocherie, 1991), which permit a clear distinction from the evolved products of the late-tectonic granitoids.

Granitoid intrusions consist of medium- to coarse-grained rocks with hypidiomorphic equigranular and heterogranular textures, the latter containing K-feldspar megacrysts (2–10 cm). Plagioclase, perthitic K-feldspar and quartz are the main mineral phases. Plagioclase is always euhedral and, in tonalitic intrusions, displays complex zonation patterns with patchy textures. Its composition varies from An_{85} to An_{25} in tonalitic–granodioritic intrusions, and from An_{35} to An_{10} in monzogranitic–leucogranitic intrusions. Anorthite-rich compositions are commonly found in cores of patchy zoned grains in tonalites. Mafic minerals consist of euhedral biotite ± euhedral green hornblende; clinopyroxene may occur as relics enclosed within hornblende cores in tonalites. No primary muscovite nor other alumino-silicate minerals are present in the calc-alkaline granitoids. Magnetite, apatite, zircon, allanite and sphene are the most common accessory phases.

Gabbroic complexes and undifferentiated basic septa consist of medium- to coarse-grained rocks with allotriomorphic and cumulate textures. In addition to gabbroic complexes, mafic microgranular enclaves are representative of basaltic magmas injected into acid magmas and thoroughly fragmented (Zorpi *et al.*, 1991; Poli & Tommasini, 1991*b*; Tommasini, 1993). They are fine grained with hypidiomorphic heterogranular and cumulate textures. Anorthite-rich plagioclase (An_{90-60}) and brown to green hornblende are the main phases in the least evolved basic rocks, whereas plagioclase, hornblende, quartz, biotite and K-feldspar occur in the most evolved rocks, in particular in mafic microgranular enclaves. Bronzitic orthopyroxene and augitic clinopyroxene are found in some gabbroic units (e.g. Punta Falcone, Northern Sardinia); clinopyroxene also occurs as resorbed cores within hornblende grains. Olivine crystals (Fo_{70-75}) are rare and are found only in the most basic units of some gabbroic complexes (e.g. Pila Canale, South-Western Corsica). Magnetite, ilmenite, apatite and sphene are the most common accessory phases.

Selection criteria of the calc-alkaline parental magmas

A detailed sampling programme has been carried out in the SCB to place constraints on differentiation processes during magma emplacement and to permit the selection of rock samples representative of the parental mantle- and crust-derived magmas (Tommasini, 1993). The key sectors have been chosen along a north–south transverse of the Batholith (Fig. 1) to highlight possible geochemical variations of parental mantle- and crust-derived magmas. The data set, consisting of >200 samples (Tommasini, 1993), is shown in Fig. 2 with the fields of the calc-alkaline and shoshonitic associations from previous works (Orsini, 1980; Bralia *et al.*, 1982; Cocherie, 1984). The samples are representative of the main calc-alkaline intrusions and include gabbroic complexes, undifferentiated basic septa, mafic microgranular enclaves, late-tectonic I-type granitoids and post-tectonic I-type leucogranites.

Several differentiation processes, often superimposed within a single batch of magma, have been recognized on the basis of field, petrographic and geochemical characteristics of rocks outcropping in each sector (Tommasini, 1993). The spatial and temporal coexistence of partially molten basic and acid magmas determined the occurrence of several interaction processes that gave rise to the wide compositional range observed in the calc-alkaline association of the SCB (Fig. 2). As such, most samples are not representative of parental magmas directly originating from partial melting processes and cannot provide constraints on the nature and characteristics of mantle and crustal sources of the Hercynian calc-alkaline magmas. Zr vs SiO_2 is plotted in Fig. 3a to give a brief overview of the study of Tommasini (1993) and to highlight the criteria adopted for sample selection.

The light grey arrow indicates the evolutionary trend of mantle-derived magmas caused by contamination and fractional crystallization processes (CFC, Poli & Tommasini, 1991*b*). These processes produced an increase in large ion lithophile elements (LILE; e.g. Rb, K) and silica in the derivative magmas. Some examples of these hybrid rocks are reported in Table 3. They are representative of mafic microgranular enclaves, discrete tonalitic plutons, marginal portions of undifferentiated basic septa and outer units of gabbroic complexes at contacts with the enclosing granitoids. The scatter observed in Fig. 3a is in part due to having plotted in one diagram all samples from each sector studied (Fig. 1). There are, however, other processes superimposed on the dominant evolutionary mechanism. For example, the

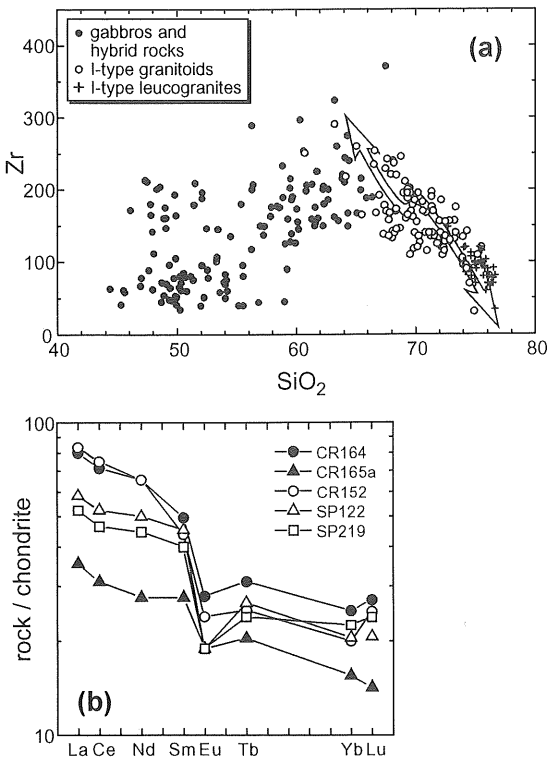

Fig. 3. (a) Zr vs SiO_2 diagram illustrating the main evolutionary processes of Hercynian magmas of the Sardinia–Corsica Batholith. The grey arrow indicates the evolution of basic magmas owing to contamination and fractional crystallization processes; the double-headed white arrow indicates the evolution of acid magmas owing to mixing–mingling processes with derivative products of basic magmas (upward trend) and crystal fractionation processes (downward trend). (b) Chondrite-normalized REE patterns of selected hybrid mantle-derived rocks that experienced amphibole accumulation.

basic samples with high Zr content (>150 p.p.m., Fig..3a) have petrographical and geochemical characteristics [e.g. rare earth element (REE) pattern, Fig. 3b] suggesting they have experienced amphibole accumulation. Despite cumulus processes, the Rb content of these basic samples is high (50–160 p.p.m., Table 3). Some of these cumulate hybrid rocks have also high K_2O contents (e.g. SP122, Table 3) and plot outside the field of the calc-alkaline association (Fig. 2b). In this case, contamination processes caused the replacement of amphibole by biotite (e.g. Johnston & Wyllie, 1988) resulting in an increase of K_2O, Rb and Ba.

The double-headed white arrow in Fig. 3a indicates the two dominant evolutionary trends of crust-derived magmas. The upward trend is caused by interaction processes between mantle- and crust-derived magmas. Mingling processes occurred between coexisting basic and acid magmas during the attainment of thermal equilibrium (Poli &

Table 3: Major (wt %) and trace element (p.p.m.) analyses of samples from the Sardinia–Corsica Batholith representative of hybrid mantle-derived magmas and a metamorphic xenolith

	Western and SW Corsica								Northern Sardinia				Central Sardinia		SW Sardinia				SW Corsica
Sample:	CR164	CR160	CR152	CR157A	CR118	CR165A	CR119	CR184	SP147	SP102	SP73	SP32	SP122	SP123	SP229	SP219	SP220	SP218	CR151
Code:	1a	1a	2a	2b	1b	2a	1b	2b	3	3	3	3	2a	4	1b	2a	4	2b	5
SiO_2	46·12	48·98	49·79	56·81	58·85	59·05	60·60	67·51	56·22	58·86	59·28	68·12	52·10	62·28	48·70	52·08	59·46	60·33	56·69
TiO_2	1·60	1·46	1·43	1·04	1·05	0·90	1·00	0·53	1·26	0·99	0·99	0·48	1·37	0·81	1·59	1·26	1·17	1·35	1·06
Al_2O_3	18·54	18·61	18·34	15·89	16·62	17·16	16·51	15·86	16·21	16·67	16·80	15·49	17·83	16·54	19·16	17·33	17·48	16·94	13·73
Fe_2O_3	12·79	11·81	10·66	9·44	6·58	7·95	6·18	4·87	3·88	2·48	2·33	0·51	2·75	1·80	11·23	11·38	7·71	7·81	7·91
FeO	—	—	—	—	—	—	—	—	5·40	5·15	4·91	3·47	7·48	4·32	—	—	—	—	–
MnO	0·14	0·12	0·12	0·14	0·07	0·09	0·07	0·08	0·16	0·13	0·14	0·10	0·16	0·10	0·11	0·13	0·09	0·07	0·15
MgO	5·26	4·33	4·27	4·16	3·74	2·98	3·23	0·95	3·42	2·95	2·45	0·85	4·28	2·26	4·41	3·88	2·16	2·23	8·20
CaO	10·00	8·49	8·42	6·53	4·84	6·66	4·54	2·43	7·07	6·19	5·63	2·74	5·82	4·39	8·57	7·50	5·32	4·58	4·36
Na_2O	2·93	3·23	3·64	3·34	4·42	3·15	4·39	4·69	2·83	2·90	3·11	3·88	3·00	3·04	2·39	3·43	2·00	3·15	2·34
K_2O	1·26	1·58	1·77	1·88	2·47	1·57	2·22	2·30	2·64	2·10	2·99	3·03	3·35	2·85	1·67	2·10	2·95	2·43	4·22
P_2O_5	0·38	0·37	0·37	0·13	0·40	0·22	0·37	0·17	0·17	0·17	0·20	0·19	0·27	0·20	0·35	0·28	0·25	0·30	0·71
LOI	0·99	1·03	1·20	0·65	0·95	0·27	0·89	0·60	0·74	1·41	1·17	1·13	1·59	1·42	1·83	0·63	1·40	0·81	0·62
ASI																			0·94
Sc	40	34	32	—	15	21	—	10·1	—	20	23	10·7	32	17	32	32	24	21	17
V	303	271	280	273	107	165	99	36	210	166	169	41	253	106	254	230	145	151	130
Cr	64	19	25	12	105	36	96	2	—	—	—	—	20	41	27	39	43	12	520
Co	33	24	22	19·4	14·2	15·2	16·4	6·9	23	18	17	6	27	14	24	23	15	14	27
Ni	17	12	8	7	40	10	37	2	10	5	5	5	17	15	12	14	16	11	225
Cu	33	30	13	31	26	14	21	3	—	—	—	—	32	12	15	29	16	16	4
Zn	134	126	115	129	88	99	86	104	—	—	—	—	140	92	127	158	93	112	198
Ga	25	25	22	22	21	18	20	29	—	—	—	—	24	22	24	24	21	20	23
Rb	53	65	81	103	138	70	138	219	81	85	109	140	163	133	74	145	117	153	370

(continued on next page)

Table 3: continued

	Western and SW Corsica								Northern Sardinia				Central Sardinia		SW Sardinia				SW Corsica
Sample:	CR164	CR160	CR152	CR157A	CR118	CR165A	CR119	CR184	SP147	SP102	SP73	SP32	SP122	SP123	SP229	SP219	SP220	SP218	CR151
Code:	1a	1a	2a	2b	1b	2a	1b	2b	3	3	3	3	2a	4	1b	2a	4	2b	5
Sr	333	318	332	170	703	277	638	79	283	262	226	146	216	219	351	189	289	201	189
Y	57	39	41	40	23	36	22	45	26	37	62	71	46	23	43	45	35	24	36
Zr	172	175	193	44	233	125	254	368	117	189	159	241	196	204	250	188	202	297	259
Nb	20	13	13	17	18	13	18	23	13	15	19	22	15	13	16	19	12	18	20
Ba	352	507	404	249	890	463	706	268	461	700	608	474	825	660	661	286	776	553	716
Hf	4·5	4·0	5·1	—	5·0	2·7	—	10·2	—	3·9	4·0	7·5	5·1	5·2	5·7	4·6	4·9	6·8	5·9
Ta	0·61	0·74	0·65	—	1·20	0·53	—	2·20	—	0·55	1·20	1·50	1·10	0·87	0·89	1·24	0·84	0·98	1·19
Pb	10	9	12	15	20	12	21	22	—	—	—	—	11	16	13	20	17	14	13
Th	1·4	1·5	2·5	—	10·5	1	—	13·3	—	3·6	8	21	1·8	11·3	2·9	1·8	10·8	14·1	23
La	24	22	25	—	49	10·6	—	13	24	23	26	54	17·5	38	31	15·7	37	56	26
Ce	60	57	63	—	89	26	—	26	59	44	65	108	44	74	67	39	74	104	62
Nd	38	33	38	—	30	16	—	15	—	22	29	41	29	30	37	26	35	38	34
Sm	10·4	8·2	9·2	—	7·4	5·8	—	4·6	—	7·4	7·3	7·9	9·5	6·5	9·3	8·4	8·0	7·3	10·0
Eu	2·06	2·00	1·77	—	1·70	1·40	—	0·58	—	1·28	1·30	0·85	1·40	1·40	1·77	1·40	1·51	1·16	2·12
Tb	1·52	0·99	1·23	—	0·68	1·00	—	0·90	—	0·78	0·95	0·96	1·30	0·67	1·18	1·17	0·90	0·73	1·03
Yb	5·0	4·2	4·0	—	1·8	3·1	—	1·7	—	2·9	4·2	5·3	4·1	2·0	3·5	4·5	3·2	2·0	2·9
Lu	0·84	0·69	0·77	—	0·39	0·44	—	0·71	—	0·41	0·77	0·90	0·64	0·32	0·53	0·74	0·46	0·31	0·57
Eu/Eu*	0·70	0·97	0·71	—	0·99	0·78	—	0·36	—	1·10	0·92	0·74	0·53	0·89	0·71	0·61	0·76	0·66	0·87
$(Tb/Yb)_n$	1·24	0·96	1·26	—	1·54	1·32	—	2·16	—	0·72	0·68	0·44	1·29	1·37	1·38	1·05	1·16	1·48	1·45
ΣREE	176	153	172	—	201	85	—	80	—	121	160	249	136	173	180	123	185	233	164

Analytical methods: whole-rock analyses were performed at the University of Perugia and Firenze. Major elements by X-ray fluorescence (XRF) after Franzini & Leoni (1972), except MgO and Na_2O which are by atomic absorption, and FeO by titration. Rare earth elements and Sc, Hf, Ta, Th are by instrumental neutron activation analysis after Poli *et al.* (1977); other trace elements by XRF after Kaye (1965). Precision is better than 5% for La, Ce, Sm, Sc, Co, Ni, Zn, Rb, Sr, Hf and Th; better than 10% for Eu, Yb, Lu, Cr, Cu, Y, Zr and Ta; better than 15% for Nd, Tb, V, Ga, Nb, Ba and Pb.

ASI, alumina saturation index [Al/(Ca+Na+K) mol %]. —, not determined

Codes—1, marginal portions of undifferentiated septa with cumulate texture (a) and non-cumulate texture (b); 2, mafic microgranular enclaves with cumulate texture (a) and non-cumulate texture (b); 3, outer units of gabbroic complexes; 4, tonalitic plutons; 5, metamorphic xenolith enclosed in granitoids.

JOURNAL OF PETROLOGY VOLUME 36 NUMBER 5 OCTOBER 1995

Tommasini, 1991*b*). Mixing processes occurred between derivative products of basic magmas thermally equilibrated and acid magmas (e.g. Frost & Mahood, 1987; Frost & Lindsay, 1988; Poli & Tommasini, 1991*b*). The downward trend is mainly caused by closed-system differentiation processes such as crystal fractionation of mafic minerals, feldspar and accessory phases (e.g. zircon, Fig. 3a). The post-tectonic leucogranites exhibit only the downward trend (Fig. 3a) because they do not have any field evidence, i.e. mafic microgranular enclaves, of interaction processes with basic magmas.

The detailed petrogenetic study of Tommasini (1993) permits a careful screening of samples from each sector of the Batholith, discarding those that experienced modification because of interaction and fractionation processes. Interaction processes (Fig. 3) are responsible for the formation of tonalitic plutons, mafic microgranular enclaves and outer units of gabbroic complexes. Basic samples have, therefore, been chosen among those of the inner units of gabbroic complexes. Major and trace element and isotopic compositions of these samples are presented in Tables 4 and 5.

In the case of the Punta Falcone gabbroic complex, for example, Tommasini & Poli (1992) demonstrated that interaction processes occurred only along contacts with the adjacent granitoid pluton, whereas the inner units did not experience interaction processes and are formed by cumulate rocks and rocks having liquid-like characteristics. The selection of cumulate rocks from the Punta Falcone gabbroic complex (Table 5) has been included only to discuss their Sr and Nd isotopes and not trace element composition and ratios, for which we refer to samples with liquid-like characteristics (Table 4). Samples from the gabbroic complexes of Ajaccio, Pila Canale and Villasimius (Table 4, Fig. 1) have been selected on the basis of a study similar to that of Tommasini & Poli (1992). The selected samples have neither cumulate textures (e.g. adcumulate texture) nor geochemical characteristics of cumulates such as significant positive Eu anomaly (e.g. $Eu/Eu^* = 2{\cdot}6$, sample PC4 from Pila Canale; Cocherie *et al.* 1994). The samples from the Pila Canale gabbroic complex (Table 4) provide independent evidence of the good quality of our selection in that their geochemical characteristics are consistent with those of the sample identified by Cocherie *et al.* (1994) as representative of parental mantle-derived liquid.

Interaction processes have been also responsible for the upward evolutionary trend of crust-derived magmas (Fig. 3a). In addition to interaction processes, closed-system evolution occurred within each magma batch (downward trend, Fig. 3a). We have therefore selected acid magmas from each sector of the Batholith (Fig. 1) on a twofold basis: (1) field (i.e. no mafic microgranular enclaves) and geochemical (e.g. Fig. 3a) evidence for the absence of interaction processes; (2) geochemical evidence for fingerprinting evolutionary processes within a single pluton, such as increase of SiO_2, decrease of Sr because of feldspar fractionation, decrease and flattening of light REE patterns owing to fractionation of accessory phases, etc. Major and trace element and isotopic compositions of the selected acid samples are presented in Tables 4 and 5.

The chosen gabbros and granitoids are considered representative of the parental mantle- and crust-derived magmas produced during the Hercynian igneous activity in Sardinia and Corsica. The selected gabbros (Table 4) have silica contents ranging from 48 to 52 wt%, and belong to normal calc-alkaline suites ($K_2O = 0{\cdot}4$–$1{\cdot}2$ wt%). The selected granitoids consist of late- and post-tectonic I-type intrusions (Table 4), have silica contents ranging from 67 to 72 wt%, and from 74 to 76 wt%, respectively, and belong to high-K calc-alkaline suites ($K_2O = 3$–5 wt%). A significant overlap in initial Sr and Nd isotope compositions is observed between the selected samples (Table 5). Gabbros have $^{87}Sr/^{86}Sr_{300\,Ma}$ and $^{143}Nd/^{144}Nd_{300\,Ma}$ values of 0·7046–0·7083 and 0·5123–0·5120, respectively; whereas granitoids have $^{87}Sr/^{86}Sr_{300\,Ma}$ and $^{143}Nd/^{144}Nd_{300\,Ma}$ values of 0·7063–0·7089 and 0·5121–0·5119, respectively. No isotopic compositions have been determined in post-tectonic leucogranites, even though available Sr isotope data (Cocherie, 1984; Beccaluva *et al.*, 1985) indicate initial compositions similar to those of the late-tectonic intrusions.

In Tables 3 and 5 we have also reported the major and trace element and isotopic composition of a metamorphic xenolith (CR 151) from South-Western Corsica, enclosed in a granitoid pluton. The sample has a granoblastic foliated texture with quartz–plagioclase (An_{40}) and phlogopite–actinolite layers. The mineral assemblage indicates an amphibolite facies metamorphism. No alumino-silicate mineral is present in the xenolith. This fact, along with other geochemical characteristics (e.g. $ASI = 0{\cdot}94$; Table 3), suggests formation from an igneous protolith. The xenolith was incorporated into the granite magma during its ascent through the crust. We are not able to establish the actual depth of provenance of the xenolith, but it is probably representative of middle–lower crust levels because the depth of emplacement of granite magmas in this sector of the Batholith was 3–4 kbar (e.g. Rossi &

Table 4: Major (wt %) and trace element (p.p.m.) analyses of the selected gabbros and granitoids of the calc-alkaline association of the Sardinia–Corsica Batholith

	Gabbros										Late-tectonic granitoids						
	Ajaccio (Iles Sanguinaires, W Corsica)		Pila Canale, SW Corsica		Punta Falcone, N Sardinia		Villasimius, SE Sardinia				Piana–Ajaccio, W Corsica			Golfe de Valinco, SW Corsica			
Sample:	CR136	CR130	CR173	CR172	SP79	SP98	SP97	SP200	SP230	SP236	CR110	CR124	CR142	CR169	CR166	CR156	CR178
SiO_2	49·58	51·95	48·99	48·03	49·69	50·50	50·76	48·85	47·59	47·88	68·04	69·12	71·94	69·35	69·75	69·78	69·83
TiO_2	0·65	0·85	1·13	1·31	1·30	1·38	1·23	1·19	0·87	0·98	0·46	0·56	0·42	0·53	0·47	0·42	0·46
Al_2O_3	16·69	16·60	17·47	18·54	18·75	18·80	18·99	16·50	17·87	16·02	15·80	14·69	13·94	14·85	15·51	15·29	14·72
Fe_2O_3	9·68	10·39	10·05	8·92	3·94	4·01	3·38	10·61	9·59	10·59	3·26	2·99	2·74	3·85	3·09	3·34	3·53
FeO	—	—	—	—	6·91	5·81	6·35	—	—	—	—	—	—	—	—	—	—
MnO	0·11	0·13	0·09	0·09	0·14	0·13	0·14	0·12	0·10	0·10	0·06	0·05	0·06	0·06	0·06	0·06	0·07
MgO	7·29	5·33	7·29	8·15	4·60	4·10	4·51	7·95	7·06	8·93	1·39	1·42	0·96	0·98	1·00	0·99	1·13
CaO	12·12	10·01	10·73	10·91	10·57	9·13	10·40	9·16	12·65	10·74	2·98	2·34	2·22	2·61	2·98	2·99	2·87
Na_2O	2·28	3·16	2·58	2·80	1·65	2·05	1·57	2·32	1·63	2·10	4·02	3·84	2·93	3·32	3·55	3·41	3·27
K_2O	0·53	0·63	0·43	0·44	0·95	1·25	1·16	0·79	0·80	0·47	3·01	3·76	3·85	3·84	3·21	3·22	3·38
P_2O_5	0·16	0·18	0·15	0·28	0·12	0·08	0·10	0·31	0·22	0·30	0·16	0·23	0·12	0·18	0·14	0·13	0·11
LOI	0·90	0·78	1·09	0·52	1·38	2·76	1·39	2·20	1·62	1·88	0·81	1·00	0·83	0·43	0·24	0·37	0·63
ASI											1·06	1·04	1·10	1·06	1·08	1·08	1·05
Sc	39	38	33	30	30	28	30	30	43	34	8·0	6·6	—	8·7	9·2	7·6	8·8
V	246	263	381	186	483	437	325	210	226	176	41	50	44	52	42	43	53
Cr	79	57	326	445	28	20	30	328	216	379	15	26	2	2	3	2	1
Co	32	31	47	39	33	35	31	39	30	41	5·0	6·6	4·8	6·1	6·4	5·6	6·0

JOURNAL OF PETROLOGY VOLUME 36 NUMBER 5 OCTOBER 1995

Ni	41	20	169	86	8	10	7	101	13	142	7	13	3	5	3	3	3
Cu	9	38	70	41	—	24	12	13	18	45	3	19	6	6	5	3	4
Zn	73	93	69	72	—	84	84	131	84	97	59	52	41	54	53	49	52
Ga	14	16	17	20	—	—	—	14	17	17	17	22	14	18	18	15	18
Rb	15	14	19	12	25	47	43	38	20	14	138	161	169	177	109	115	156
Sr	367	352	384	337	282	292	302	299	385	381	258	459	147	175	195	188	169
Y	15	19	12	20	15	20	19	24	24	20	21	20	25	37	28	24	24
Zr	47	40	45	112	78	85	60	161	89	142	133	211	133	188	179	162	118
Nb	5	4	4	6	8	7	5	7	5	10	11	15	11	12	9	12	10
Ba	189	285	101	126	283	196	177	298	169	247	565	861	522	855	831	735	633
Hf	1·2	1·3	1·3	2·5	1·9	2·3	1·9	3·2	2·0	2·5	3·7	5·9	—	5·8	5·2	4·3	4·1
Ta	0·30	0·30	0·19	0·41	0·27	0·40	0·50	0·51	0·24	0·47	1·60	1·50	—	1·48	0·91	0·62	1·19
Pb	10	7	7	10	11	12	12	6	7	6	25	30	21	25	20	20	21
Th	2·2	2·6	1·0	1·6	3·6	2·8	3·6	2·9	1·6	2·4	12·0	33	—	15·4	9·7	12·7	19·2
La	7·1	10·6	6·6	10·8	13·0	14·0	14·3	23·3	13·4	20·1	28·0	53	—	52	35	42	50
Ce	15·2	21·0	14·2	23·0	25·0	28·0	30	45	26·4	40	60	108	—	100	67	68	91
Nd	8·0	12·0	8·6	15·1	12·0	14·0	16·0	23·8	14·6	19·8	21·0	34	—	43	28	28	33
Sm	2·4	3·5	2·3	4·1	3·2	3·0	3·2	6·0	4·2	4·8	4·6	6·9	—	7·6	5·6	5·9	5·5
Eu	0·80	0·90	0·81	1·20	0·85	1·04	0·98	1·34	1·04	1·20	1·00	1·20	—	1·21	1·18	0·93	0·98
Tb	0·47	0·40	0·45	0·44	0·47	0·40	0·50	0·73	0·55	0·46	0·49	0·66	—	1·05	0·77	0·70	0·72
Yb	2·0	2·1	1·3	2·2	1·8	1·5	1·5	2·2	2·0	1·8	1·5	1·5	—	3·2	2·3	1·9	2·6
Lu	0·22	0·25	0·21	0·27	0·3	0·21	0·22	0·35	0·32	0·32	0·27	0·29	—	0·59	0·54	0·36	0·53
Eu/Eu*	1·04	1·07	1·05	1·25	0·94	1·29	1·03	0·85	0·93	1·10	0·89	0·73	—	0·57	0·76	0·60	0·67
$(Tb/Yb)_n$	0·96	0·78	1·41	0·82	1·10	1·13	1·36	1·34	1·15	1·04	1·33	1·80	—	1·34	1·37	1·50	1·13
ΣREE	47	61	44	64	68	72	79	121	76	101	131	227	—	237	161	167	206

Table 4: continued

	Late-tectonic granitoids														Post-tectonic leucogranites				
	Punta Falcone, N Sardinia							Serra di Orotelli, Central Sardinia		Villasimius, SE Sardinia					Coti Chiavari, SW Corsica		Mte Pulchiana, N Sardinia		
Sample:	SP55	SP45	SP85	SP58	SP56	SP40	SP158	SP114	SP116	SP239	SP237	SP231	SP241	SP233	CLB69	CLB68	N115	N120	N121
SiO_2	69·50	70·58	70·88	71·34	72·20	72·30	72·49	68·31	68·37	66·97	67·40	67·55	67·75	67·82	75·09	75·23	75·87	74·61	74·93
TiO_2	0·47	0·42	0·28	0·40	0·24	0·27	0·28	0·46	0·47	0·58	0·53	0·51	0·48	0·52	0·23	0·23	0·24	0·38	0·34
Al_2O_3	15·23	14·91	15·96	14·55	15·48	14·54	14·41	15·44	15·54	15·91	15·98	16·04	15·93	15·62	13·40	13·27	12·93	13·31	13·44
Fe_2O_3	0·85	0·71	0·94	1·14	0·88	0·82	1·08	1·07	1·24	4·50	4·16	4·02	3·76	4·08	2·32	2·08	0·40	0·63	0·45
FeO	2·20	2·08	1·40	1·70	1·28	1·56	1·39	2·20	2·24	—	—	—	—	—	—	—	1·08	0·92	0·94
MnO	0·06	0·06	0·06	0·06	0·06	0·08	0·08	0·06	0·07	0·07	0·06	0·06	0·06	0·06	0·07	0·07	0·05	0·05	0·05
MgO	0·91	0·85	0·48	0·61	0·32	0·51	0·48	0·94	0·95	1·28	1·17	1·18	1·13	1·20	0·29	0·24	0·21	0·20	0·19
CaO	2·72	2·42	2·14	2·11	2·51	1·95	2·11	2·92	3·03	3·57	3·55	3·44	3·32	3·13	1·38	1·44	1·16	1·24	1·29
Na_2O	3·18	3·10	3·11	3·11	3·13	3·46	3·40	3·39	3·58	3·37	3·47	3·50	3·37	3·28	3·24	3·48	2·97	2·84	2·98
K_2O	3·91	3·98	4·25	4·14	3·22	3·68	3·73	3·87	3·67	2·95	2·87	3·01	3·45	2·88	4·10	4·10	4·41	5·11	4·86
P_2O_5	0·14	0·09	0·05	0·11	0·11	0·12	0·09	0·16	0·16	0·20	0·18	0·17	0·16	0·17	—	—	0·04	0·05	0·05
LOI	0·82	0·80	0·45	0·73	0·56	0·73	0·46	1·18	0·69	0·59	0·63	0·53	0·60	1·22	0·48	0·44	0·63	0·66	0·48
ASI	1·08	1·10	1·18	1·10	1·20	1·12	1·09	1·05	1·04	1·08	1·08	1·08	1·07	1·13	1·09	1·04	1·11	1·08	1·09
Sc	9·0	8·5	5·6	7·5	4·5	5·0	5·1	7·0	8·5	—	9·1	—	11·3	9·3	5·0	4·7	4·6	3·9	4·5
V	—	—	—	—	—	—	—	49	46	71	68	64	60	65	—	—	16	15	12
Cr	10	15	—	—	2	—	—	11	13	4	4	4	2	4	—	—	—	—	—
Co	6·7	6·4	4·8	4·5	2·6	2·5	2·8	6·0	4·0	7·5	8·0	8·1	7·0	8·2	3·3	3·7	2·7	2·0	2·4
Ni	—	—	—	—	—	—	—	5	5	8	8	8	9	8	—	—	5	5	7

JOURNAL OF PETROLOGY VOLUME 36 NUMBER 5 OCTOBER 1995

Cu	—	—	—	—	—	—	—	5	4	6	5	5	5	4	—	—	4	4	3
Zn	—	—	—	—	—	—	—	59	60	66	74	64	58	64	42	38	36	30	29
Ga	—	—	—	—	—	—	—	22	21	20	16	16	18	21	—	—	24	22	26
Rb	136	136	141	163	129	138	149	165	157	126	131	134	135	133	190	206	151	130	132
Sr	204	184	155	161	185	164	168	189	202	184	190	187	187	184	66	68	55	85	72
Y	32	30	28	40	30	35	25	18	19	26	21	26	21	26	—	—	24	18	23
Zr	202	183	168	197	120	136	129	170	173	192	178	170	158	168	133	130	103	107	98
Nb	14	15	13	17	15	20	11	12	13	10	11	9	8	10	—	—	8	4	15
Ba	1010	855	789	760	538	570	535	639	645	567	603	629	812	592	451	410	305	634	502
Hf	4·8	4·5	3·9	4·7	3·1	3·2	3·4	5·3	4·9	—	4·2	—	3·9	5·1	3·8	3·8	3·6	3·6	3·6
Ta	0·94	0·91	0·87	1·10	1·10	1·00	1·20	0·70	0·88	—	0·88	—	0·70	0·80	2·28	2·22	0·94	0·49	0·85
Pb	—	—	—	—	—	—	—	24	23	21	18	21	24	20	—	—	25	23	27
Th	11·6	11·6	13·4	14·7	10·3	10·9	11·0	9·4	11·7	—	11·0	—	14·4	12·0	18·8	16·2	33	18·2	15·8
La	48	38	39	39	28·0	25·0	27·0	20·8	29·8	—	31	—	46	33	29·2	30	31	41	35
Ce	93	71	74	81	54	49	56	41	57	—	54	—	83	62	56	57	69	89	68
Nd	44	33	24·0	29	22·0	16·1	25·0	18·0	20·0	—	23·8	—	31	25·0	—	—	28	37	25
Sm	6·0	5·2	4·2	5·4	3·9	4·7	4·7	3·6	4·9	—	4·6	—	5·7	4·3	4·8	5·0	6·0	5·5	5·4
Eu	1·30	1·10	0·90	0·95	0·87	0·76	0·80	0·95	1·09	—	1·00	—	1·08	0·94	0·63	0·70	0·53	0·81	0·70
Tb	0·80	0·62	0·66	0·65	0·60	0·52	0·71	0·50	0·52	—	0·54	—	0·71	0·51	0·82	0·81	0·76	0·57	0·53
Yb	2·5	2·2	2·2	2·1	2·4	2·6	2·7	1·7	1·8	—	2·0	—	1·9	2·1	3·3	3·4	2·5	2·1	2·1
Lu	0·41	0·34	0·38	0·30	—	0·40	—	0·24	0·34	—	0·32	—	0·34	0·33	—	—	0·55	0·29	0·34
Eu/Eu*	0·79	0·83	0·73	0·68	0·78	0·68	0·60	0·95	0·92	—	0·86	—	0·70	0·88	—	—	0·33	0·62	0·57
$(Tb/Yb)_n$	1·31	1·15	1·22	1·26	1·02	0·82	1·07	1·20	1·18	—	1·13	—	1·57	0·97	—	—	1·24	1·11	1·03
ΣREE	219	170	164	178	128	114	136	100	130	—	132	—	190	144	—	—	159	195	154

Analytical methods as in Table 3. ASI, alumina saturation index [Al/(Ca + Na + K) mol%]. —, not determined.
Samples of Punta Falcone are from Poli & Tommasini (1991*a*) and Tommasini & Poli (1992); samples of Coti Chiavari are from Cocherie (1984).

Table 5: Sr and Nd isotope data of the selected gabbros and granitoids of the calc-alkaline association of the Sardinia–Corsica Batholith

Location	Sample	Rb (p.p.m.)	Sr (p.p.m.)	Rb/Sr (wt)	$^{87}Rb/^{86}Sr$ (atomic)	$^{87}Sr/^{86}Sr_{meas}$ (atomic)	$^{87}Sr/^{86}Sr_{300Ma}$ (atomic)	Nd (p.p.m.)	Sm (p.p.m.)	Sm/Nd (wt)	$^{147}Sm/^{144}Nd$ (atomic)	$^{143}Nd/^{144}Nd_{meas}$ (atomic)	$^{143}Nd/^{144}Nd_{300Ma}$ (atomic)
Gabbros													
SW Corsica	CR172	10·8	337·6	0·03211	0·09288	0·704999 ± 14	0·70460 ± 2	15·25	3·848	0·2523	0·1526	0·512595 ± 10	0·512295 ± 10
N Sardinia	SP96*	18·4	223·1	0·08265	0·2391	0·708995 ± 31	0·70797 ± 3	9·568	2·534	0·2648	0·1601	0·512304 ± 9	0·511990 ± 9
N Sardinia	SP39*	12·1	299·3	0·04036	0·1168	0·708695 ± 17	0·70820 ± 2	8·973	2·147	0·2393	0·1447	0·512281 ± 9	0·511997 ± 9
N Sardinia	SP77*	26·1	381·4	0·06833	0·1978	0·709182 ± 21	0·70834 ± 2	9·733	2·146	0·2205	0·1333	0·512245 ± 10	0·511983 ± 10
SE Sardinia	SP230	17·5	357·4	0·04905	0·1419	0·707301 ± 14	0·70670 ± 2	15·24	3·704	0·2430	0·1469	0·512325 ± 9	0·512036 ± 9
Granitoids													
W Corsica	CR110	132	258·5	0·5114	1·481	0·713668 ± 10	0·70735 ± 6	23·23	4·599	0·1980	0·1186	0·512302 ± 9	0·512069 ± 9
W Corsica	CR183†	239	74·77	3·191	9·266	0·745857 ± 13	0·7063 ± 4	24·14	5·209	0·2158	0·1205	0·512271 ± 9	0·512034 ± 9
SW Corsica	CR166	106	195·7	0·5422	1·571	0·714669 ± 13	0·70797 ± 7	30·66	5·943	0·1938	0·1172	0·512250 ± 10	0·512020 ± 10
SW Corsica	CR167†	165	104·7	1·580	4·578	0·726676 ± 10	0·7071 ± 2	29·96	5·544	0·1850	0·1119	0·512273 ± 9	0·512053 ± 9
N Sardinia	SP55	131	200·8	0·6529	1·891	0·716139 ± 13	0·70807 ± 8	36·77	6·221	0·1692	0·1023	0·512247 ± 8	0·512046 ± 8
N Sardinia	SP58	155	156·6	0·9911	2·872	0·720584 ± 15	0·7083 ± 1	31·90	5·860	0·1837	0·1111	0·512234 ± 8	0·512016 ± 8
Central Sardinia	SP116	146	196·5	0·7450	2·159	0·717804 ± 10	0·70859 ± 9	23·97	4·724	0·1971	0·1191	0·512180 ± 9	0·511946 ± 9
Central Sardinia	SP109†	237	99·11	2·386	6·924	0·737738 ± 10	0·7082 ± 3	25·58	5·053	0·1975	0·1194	0·512184 ± 10	0·511950 ± 10
SE Sardinia	SP237	128	186·6	0·6860	1·986	0·717457 ± 10	0·70898 ± 9	21·75	4·186	0·1925	0·1163	0·512206 ± 8	0·511978 ± 8
SE Sardinia	SP241	128	185·0	0·6919	2·004	0·717325 ± 13	0·70877 ± 9	29·97	5·265	0·1757	0·1062	0·512168 ± 10	0·511959 ± 10
Metamorphic xenolith													
SW Corsica	CR151	346	180·7	1·917	5·558	0·730271 ± 13	0·7065 ± 2	42·70	9·234	0·2163	0·1307	0·512333 ± 09	0·512076 ± 9

Analytical methods described in Appendix 1. Uncertainties in measured and initial isotopic ratios refer to least significant digits and represent $\pm 2\sigma$ run precision and $\pm 2\sigma$ error propagation, respectively.
Initial Sr and Nd isotopes have been calculated at 300 Ma on the basis of the mean age of the calc-alkaline association in the Sardinia–Corsica Batholith (Cocherie, 1984; Beccaluva *et al.*, 1985). An amphibolite facies meta-igneous xenolith enclosed in granitoid plutons from South-Western Corsica has been also analysed.
*Cumulate rock samples. †Evolved rock samples.

JOURNAL OF PETROLOGY VOLUME 36 NUMBER 5 OCTOBER 1995

Cocherie, 1991). The geochemical and isotopic characteristics of this sample will be taken into account in the following discussion on the genesis of parental mantle- and crust-derived magmas selected from the data set of Tommasini (1993).

PETROGENESIS OF PARENTAL MANTLE-DERIVED MAGMAS

The selected gabbroic samples representative of the parental mantle-derived magmas in the different sectors of the SCB have major and trace element characteristics typical of high-alumina calc-alkaline basalts (e.g. Perfit *et al.*, 1980; Pearce, 1982). They plot in the calc-alkaline basalt field in the Th/Yb vs Ta/Yb diagram (Fig. 4), and have high Al_2O_3 content (Table 4), high large ion lithophile element (LILE) vs high field strength element (HFSE) ratios (e.g. Th/Ta = 4–13), and concave upward REE patterns (La/Sm = 2·9–4·7). The calc-alkaline affinity is also evident from the relative Nb and Ta depletions in primitive mantle-normalized diagrams (Fig. 5). Figure 5 also shows a marked relative enrichment in Rb, Ba, K and Pb. Two main processes could be responsible for the enrichment in lithophile elements and the high Th/Yb values: (1) interaction between crustal material and basic magmas during their ascent in the crust (e.g. Hildreth & Moorbath, 1988; Wilson, 1989); (2) enrichment of the mantle source of basic magmas by recycling of crustal material (e.g. Gill, 1981; Sun & McDonough, 1989; Wilson, 1989).

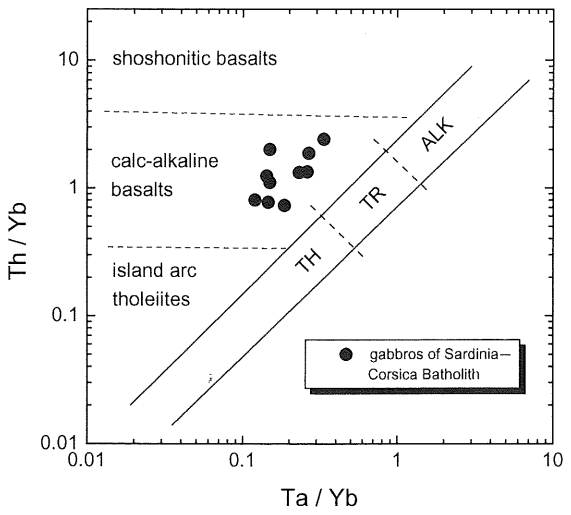

Fig. 4. Th/Yb vs Ta/Yb discrimination diagram (Pearce, 1982) of the selected gabbros from the Sardinia–Corsica Batholith showing their calc-alkaline affinity. TH, tholeiitic basalts; TR, transitional basalts; ALK, alkaline basalts.

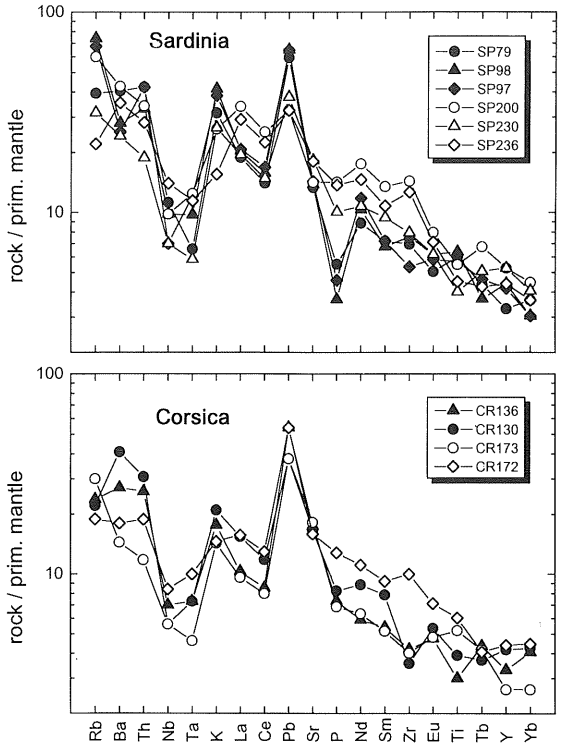

Fig. 5. Primitive mantle-normalized diagrams (Sun & McDonough, 1989) of the selected gabbros from the Sardinia–Corsica Batholith.

Interaction of basic magmas with crustal material

Interaction of basic magmas with crustal material *en route* to the surface could have been important in that none of the selected gabbros are primitive melts in equilibrium with mantle sources (e.g. Perfit *et al.*, 1980). Their ferromagnesian element contents (e.g. Ni, Cr; Table 3) indicate olivine and pyroxene fractionation. Conservative estimates on the basis of average Ni and Cr partition coefficients in olivine and pyroxenes (Henderson, 1986) allow a maximum value of solid removal of ~30–35%. This upper limit is reduced if assimilation of crustal materials with low Ni and Cr contents occurred. A number of likely crustal contaminants from the SCB, the French Massif Central and the Ivrea Zone have been taken into account to test this hypothesis. The rationale of considering crustal components from the French Massif Central and the Ivrea Zone is based on the Late Palaeozoic position of Sardinia and Corsica close to Southern France (e.g. Auzende *et al.*, 1973; Westphal *et al.*, 1976; Edel *et al.*, 1981). Average compositions of these groups of crustal material are reported in Table 6, along with the hypothetical composition of the uncontaminated basic magma.

We have tried several assimilation–fractional crystallization (AFC) models to find a match for the isotopic and trace element composition of the selected gabbros. Assuming a fractionating mineral assemblage composed of olivine, pyroxene and plagioclase, the bulk distribution coefficients (D) for Rb, Sm and Nd have been kept constant at conservative high values of 0·1, 0·5 and 0·3, respectively [see average K_d of Henderson (1986)]. D^{Sr} has been varied from 1·4 to 1·1 and 0·8, corresponding to an amount of plagioclase in the fractionating mineral assemblage of ~80%, 60% and 45%, respectively (average $K^{Sr}_{d\,plag} = 1{\cdot}8$; Henderson, 1986). High rates of assimilation vs crystallization ($r = 0{\cdot}6$–$0{\cdot}8$) are demanded in each case to achieve the Sr and Nd isotope composition of the selected gabbros. This is a consequence of the similar Sr content in the basic magma and assimilated material. Such high r values cause the Rb content of the derivative liquids to increase in most cases to >80–100 p.p.m. High Rb content is observed in the hybrid basic samples of the SCB even in the case of cumulates (Table 3), but is not consistent with the Rb content of the selected gabbros (12–47 p.p.m., Table 4). Moreover, rough estimates on the basis of SiO_2 and K_2O contents of the hypothetical assimilated crustal materials indicate significantly higher values of these elements in the modelled derivative liquids than those observed in the selected gabbros.

There is a group of crustal materials (group 7, Table 6), however, that deserves a separate treatment. Group 7 represents lower-crust metasedimentary granulite xenoliths without Al_2SiO_5 (Downes *et al.*, 1990). Assimilation of this type of low-Rb crustal material might be consistent with the isotopic and trace element composition of the selected gabbros, even though the result still indicates a rather high Rb content in the modelled derivative liquids (~40 p.p.m. at $^{87}Sr/^{86}Sr = 0{\cdot}7076$ and ~60 p.p.m. at $^{87}Sr/^{86}Sr = 0{\cdot}7090$). Lower-crust material with low Rb content is also likely to have low Th content (e.g. Wilson, 1989). Th data are available only for two of the group 7 samples (1·3 and 0·2 p.p.m.; Downes *et al.*, 1990). Their Th/Yb values are 0·3 and 0·1, in keeping with estimates for lower-crust granulites (Th = 0·42 p.p.m., Th/Yb = 0·35; Weaver & Tarney, 1981). Assimilation of this material is not consistent with the Th/Yb values of the selected gabbros (Fig. 4), which suggest assimilation of upper-crust material (e.g. Th = 10 p.p.m., Th/Yb = 4·9; Taylor & McLennan, 1985) such as, for example, groups 1, 2, 3 and 8 (Table 6). Assimilation of these latter crustal materials is, however, ruled out on the basis of the Rb content of the modelled derivative liquids. This

Table 6: Average composition of crustal material forming the pre-Hercynian basement of Western Europe (groups 1–8) and hypothetical composition of the basic magma used in the AFC calculation

Group	Lithotype	Ref.	SiO_2	K_2O	Rb	Sr	$^{87}Sr/^{86}Sr_{300Ma}$	Sm	Nd	$^{143}Nd/^{144}Nd_{300Ma}$
1	Orthogneiss	1	66·8	3·8	149	175	0·71399			
2	Augen-gneiss	1			239	48	0·74868			
3	Orthogneiss	2	74·6	4·6	233	59	0·75172	4·2	17·6	0·51195
4	Lower-crust kinzigite	3			86	220	0·71559	7·4	39·4	0·51178
5	Lower-crust metaigneous xenolith	4	63·7	2·0	47	333	0·70936	6·1	34·4	0·51195
6	Lower-crust metasedimentary xenolith	4	63·1	3·0	63	184	0·71616	7·6	41·2	0·51189
7	Lower-crust metasedimentary xenolith w/o Al_2SiO_5	4	59·6	1·3	34	301	0·71189	4·8	21·4	0·51189
8	Metasediment	5			144	157	0·71907	6·8	40·3	0·51164
	Basic magma		47·0	0·1	6–8	300–600	0·704	2·4	10	0·5126

Data sources: 1, Beccaluva *et al.* (1985); 2, Downes & Duthou (1988); 3, Voshage *et al.* (1990); 4, Downes *et al.* (1990); 5, Turpin *et al.* (1990).

Th–Rb controversy argues against significant assimilation of crustal material by the selected gabbros.

The middle–lower crust xenolith from South-Western Corsica (CR151, Tables 3 and 5) provides further arguments against the assimilation hypothesis. Its $^{87}Sr/^{86}Sr_{300\,Ma}$, value along with its Sr content, requires high assimilation rates by basic magmas, to result in Sr isotope ratios that are significantly modified. This assimilation results, however, in drastically increasing Rb contents of the derivative magmas owing to the high Rb content in CR151 (Table 3), and does not account for the Rb content observed in the selected gabbros.

Assimilation of crustal material and fractional crystallization of basic magmas should also result in systematic correlations in Rb/Ba, Rb/Sr, Sr/Nd and Ba/Ce vs SiO_2 and MgO, whereas no such evidence is displayed by the selected gabbros (Fig. 6). Therefore, we conclude that interaction with crustal material did not modify significantly the trace element and isotopic composition of the selected gabbros during their ascent in the crust.

Enrichment of the mantle source of basic magmas by recycling of crustal material

Incompatible trace element ratios of the selected gabbros from the SCB can provide a powerful tool to assess the role of recycling of crustal material in the subcontinental mantle of Sardinia and Corsica. In general, ratios of incompatible trace elements are not fractionated during equilibrium partial melting and crystal fractionation processes (e.g. Hofmann *et al.*, 1986). In fact, even allowing a two order of magnitude difference in incompatibility between a pair of trace elements, their ratio in the melt is fractionated with respect to the source by a factor <2 for large degrees of partial melting such as those in calc-alkaline environments (Green, 1973, 1976). The same holds for the case of fractional crystallization, considering incompatible trace element ratios in the initial magma and in derivative products, for amounts of solid removal $<70\%$. Thus, incompatible trace element ratios of the selected gabbros are likely to mirror those of their sources, and can permit constraints on the geochemical characteristics of the subcontinental mantle underneath Sardinia and Corsica during the Hercynian orogeny.

In Fig. 7 we plot incompatible trace element ratios of the selected gabbros from the SCB along with protogranular spinel peridotite xenoliths from the French Massif Central and other segments of the Hercynian chain (Jagoutz *et al.*, 1979; Downes & Dupuy, 1987; Jochum *et al.*, 1989), MORB-type mantle and subcontinental lithospheric mantle estimates (Wood, 1979; Sun & McDonough, 1989; McDonough, 1990), Hercynian metasedimentary material from the French Massif Central (Downes *et al.*, 1990; Turpin *et al.*, 1990), and generic sedimentary material—shales (Taylor & McLennan, 1985; White *et al.*, 1985). In Fig. 7 we also plot other two groups of samples from the French Massif Central: (1) the mantle-derived parental magma of the Limousin quartz diorite (D1 and D3, Shaw *et al.*, 1993); (2) the granulite facies mantle-derived mafic xenoliths, scavenged by Tertiary alkaline volcanic

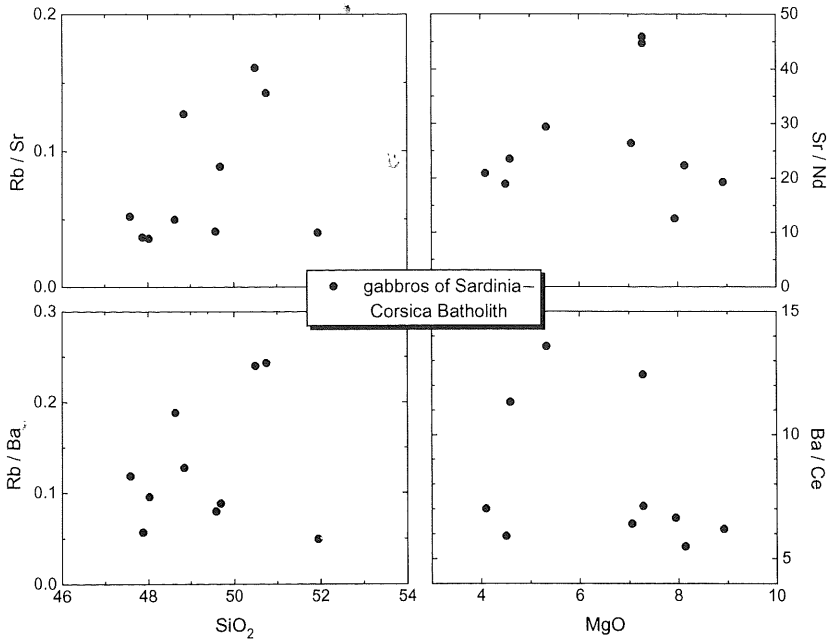

Fig. 6. Rb/Sr and Rb/Ba vs SiO_2, and Sr/Nd and Ba/Ce vs MgO of the selected gabbros from the Sardinia–Corsica Batholith.

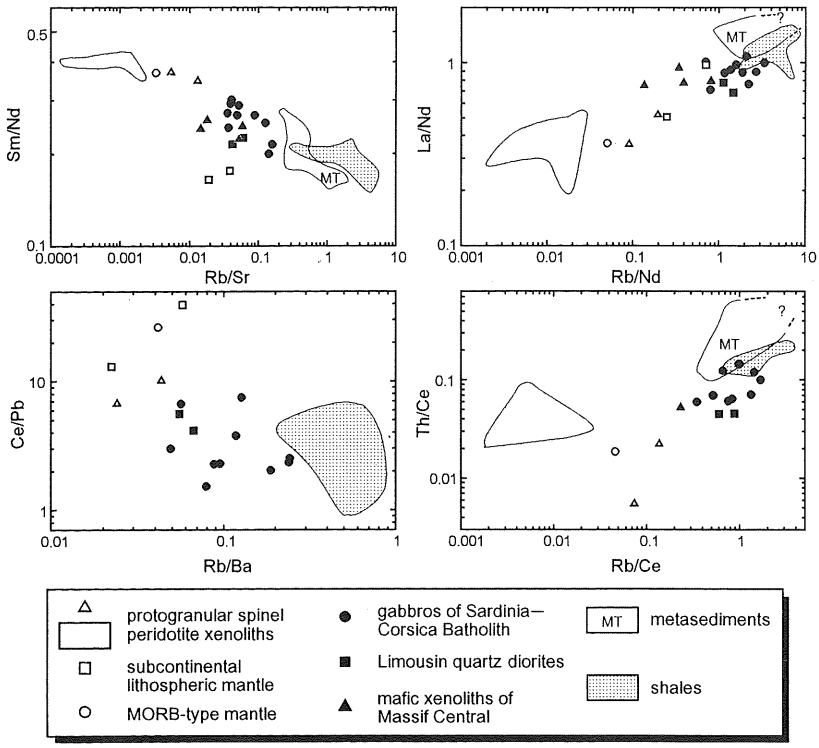

Fig. 7. Incompatible trace element ratio diagrams of the selected gabbros from the Sardinia–Corsica Batholith to place constraints on mantle source characteristics (see text). The Limousin quartz diorites are from Shaw *et al.* (1993); mafic xenoliths of the French Massif Central are from Downes *et al.* (1990) and represent mantle-derived magmas approaching liquid composition. Field of ultramafic xenoliths is on the basis of leached clinopyroxene analyses from protogranular spinel peridotite xenoliths (Downes & Dupuy, 1987); open triangles are whole-rock composition of two mantle xenoliths from Massif Central, France, and Eifel, Germany (Jagoutz *et al.*, 1979; Jochum *et al.*, 1989). Subcontinental lithospheric mantle compositions are reported for comparison and refer to mean and median composition (McDonough, 1990). MORB-type mantle composition is from Wood (1979) and Sun & McDonough (1989). Metasediment composition is from Downes *et al.* (1990) and Turpin *et al.* (1990); shale composition is from Taylor & McLennan (1985) and White *et al.* (1985).

rocks, that are considered to approach liquid compositions and to have been emplaced during the Hercynian orogeny (Downes *et al.*, 1990). In these latter samples we did not include RP8 and BAL1120 because of their high Rb content (see table II, Downes *et al.*, 1990). Caution has been paid in using trace elements that have incompatible behaviour during both mantle melting and fractional crystallization of primitive basic magmas because the selected gabbros from the SCB are not primitive magmas but have experienced ~30–35% olivine and pyroxene removal. In particular, Sr has been used as incompatible trace element because plagioclase is not present in the mineral assemblage of ultramafic xenoliths from the French Massif Central (Downes & Dupuy, 1987), and in general estimates of the modal composition of the subcontinental mantle (e.g. Wilson, 1989; McDonough, 1990). Also, the absence of systematic variations in Rb/Sr, Rb/Ba, Sr/Nd and Ba/Ce vs SiO_2 and MgO (Fig. 6) suggests that neither plagioclase nor micas have been involved in the fractional crystallization process experienced by the selected gabbros. Moreover, conservative estimates indicate that, for example, Rb/Sr in derivative magmas would vary by a factor $<2{\cdot}4$ with respect to the ratio in primitive magmas for an amount of solid removal $<50\%$, and using a $D^{Rb}=0$ and a $D^{Sr}=1{\cdot}3$, the latter corresponding to an unsupported (see the absence of correlation between Rb/Sr and SiO_2 in Fig. 6) amount of plagioclase in the fractionating mineral assemblage of ~70% and to average $K^{Sr}_{d\,plag}$ in basic magmas of 1·8 (Henderson, 1986). Other trace elements used in Fig. 7 have an actual incompatible behaviour during fractional crystallization from primitive basic magmas, and their ratios, such as La/Nd or Th/Ce, would vary by a factor $<1{\cdot}5$ for amount of solid removal $<50\%$ and allowing unreasonable mass fractions (i.e. 100%) of fractionating clinopyroxene [see average K_d values for clinopyroxene in basic magmas in Henderson (1986)].

This being the case, it can be safely concluded that incompatible trace element ratios observed in the selected gabbros (Fig. 7) resemble those of the

mantle source. The intermediate trace element ratios of the selected gabbros with respect to ultramafic xenoliths and sedimentary material (Fig. 7) could be accounted for by sediment recycling into the mantle source. Rough estimates suggest that geochemical characteristics of the mantle source can be reproduced by recycling <5 wt % sedimentary material into an average MORB-type mantle. Moreover, we must consider that mixing processes did not occur between mantle and bulk sediments but, more realistically, between mantle and partial melts of sediments. This results in a decrease in the amount of modelled sedimentary material added to the mantle because magmas produced by melting of sediments are likely to have higher ratios of certain trace elements such as Rb/Sr.

The correspondence between the composition of Hercynian mantle-derived magmas from the French Massif Central and the selected gabbros from the SCB in terms of incompatible trace element ratios (Fig. 7) suggests the occurrence of similar enrichment processes in the subcontinental mantle of Southern France. This is consistent with the conclusion of Shaw *et al.* (1993) on the genesis of the Limousin quartz diorite. Evidence for recycling of sedimentary material into the European subcontinental mantle is also provided from: (1) geochemical, isotopic and textural characteristics of spinel peridotite xenoliths from the French Massif Central (Downes & Dupuy, 1987); (2) trace element (e.g. Ce/Pb <10) and isotopic (Fig. 8) characteristics of Late Carboniferous to Early Permian lamprophyres from the French segment of the Hercynian Belt (Turpin *et al.*, 1988); (3) a recent noble gas study ($^{3}He/^{4}He$, $^{40}Ar/^{36}Ar$) of mantle xenoliths scavenged by Tertiary alkaline volcanic rocks (Dunai & Baur, 1995).

Timing of enrichment of the mantle source of basic magmas

A reasonable mechanism to explain sediment addition to the mantle is recycling of sedimentary material via subduction zones. This process is well documented in many subduction-related environments (e.g. Gill, 1981; McCulloch & Perfit, 1981; White & Patchett, 1984; White & Dupre, 1986) and is supported by ^{10}Be anomalies in modern volcanic arc basalts (e.g. Brown *et al.*, 1982). However, the Hercynian orogeny in Sardinia and Corsica has been related to a continent–continent collision geodynamic setting (e.g. Rossi & Cocherie, 1991; Carmignani *et al.*, 1992), and therefore the enrichment event in the subcontinental mantle underneath Sardinia–Corsica has to be due to earlier subduction.

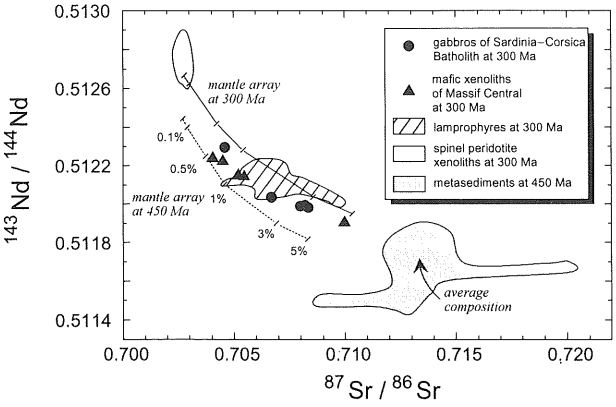

Fig. 8. $^{143}Nd/^{144}Nd$ vs $^{87}Sr/^{86}Sr$ diagram of the selected gabbros from the Sardinia–Corsica Batholith to assess the age of the enrichment event in the mantle source (see text). Mafic xenoliths of the French Massif Central are from Downes *et al.* (1990) and represent mantle-derived magmas approaching liquid composition. Field of lamprophyres of the French Massif Central is from Turpin *et al.* (1988). Field of ultramafic xenoliths at 300 Ma has been calculated from data on leached clinopyroxenes from protogranular spinel peridotite xenoliths (Downes & Dupuy, 1987). Mantle arrays at 300 and 450 Ma have been calculated from data by Faure (1986). Dashed line: mixing line between MORB-type mantle and average metasediment composition at 450 Ma with figures referring to mass fractions (wt %) of metasediments in the mixture; continuous line: isotopic composition of the enriched mantle after 150 Ma. Trace element (p.p.m.) composition of MORB-type mantle used in the mixing calculation is the average composition of protogranular spinel peridotite xenoliths (p.p.m. in clinopyroxene × modal abundance of clinopyroxene), whereas isotopic composition refers to mantle array values at 450 Ma for a MORB-type mantle: Rb = 0·006, Sr = 7·8, Sm = 0·21, Nd = 0·53, $^{87}Sr/^{86}Sr_{450\ Ma} = 0{\cdot}7027$, $^{143}Nd/^{144}Nd_{450\ Ma} = 0{\cdot}51246$. Trace element (p.p.m.) and isotopic composition of sedimentary material used in the mixing calculation is the average composition of metasediments from the French Massif Central (Downes *et al.*, 1990; Turpin *et al.*, 1990): Rb = 103, Sr = 175, Sm = 7·2, Nd = 41, $^{87}Sr/^{86}Sr_{450\ Ma} = 0{\cdot}71326$, $^{143}Nd/^{144}Nd_{450\ Ma} = 0{\cdot}51166$.

An active continental margin with subduction of oceanic crust below continental crust was proposed for the Ordovician (~450 Ma) igneous activity (e.g. Memmi *et al.*, 1983; Carmignani *et al.*, 1986, 1987, 1992) (Table 1). It is possible that recycling of sedimentary material in the Sardinia–Corsica subcontinental mantle occurred at that time.

Sr and Nd isotopes provide tests for this hypothesis. $^{87}Sr/^{86}Sr_{300\ Ma}$ and $^{143}Nd/^{144}Nd_{300\ Ma}$ values of the selected gabbros from the SCB are reported in Fig. 8, along with Hercynian granulite facies mantle-derived mafic xenoliths (Downes *et al.*, 1990), Late Carboniferous to Early Permian lamprophyres (Turpin *et al.*, 1988), and protogranular spinel peridotite xenoliths (Downes & Dupuy, 1987) from the French Massif Central. The spectrum of data deviates significantly from the mantle array at 300 Ma, as predicted for mantle sources enriched by recycled crustal material. The field of Hercynian metasedimentary material from the French Massif Central at

450 Ma is reported along with the mantle array at 450 Ma. We calculated variations in Sr and Nd isotopes in a MORB-type mantle at 450 Ma by adding the average metasediment composition (dashed line, Fig. 8). Low mass fractions of metasediments (<5 wt%) significantly modify the mantle isotopic signature. Then, we estimated the isotopic signature of the enriched MORB-type mantle after a time span of 150 Ma (continuous line, Fig. 8), i.e. during the Hercynian igneous activity (300 Ma). Variations of Sr and Nd isotopes of the enriched MORB-type mantle at 300 Ma are consistent with isotopic compositions observed in the selected gabbros from the SCB as well as in the other mantle-derived magmas from the French Massif Central (Fig. 8).

Thus, geochemical and isotopic arguments provide evidence for enrichment processes in the subcontinental mantle underneath Sardinia and Corsica through recycling of sediments via subduction zones during the Ordovician igneous activity (~450 Ma). The geochemical characteristics of the mantle source of basic magmas from the SCB can be accounted for by mixing between a MORB-type mantle, as indicated by protogranular spinel peridotite xenoliths (Downes & Dupuy, 1987), and low mass fractions (<5 wt%) of sedimentary material or acid melts originating through partial melting of sediments. Isotopic compositions of Hercynian mantle-derived magmas from the French Massif Central (Fig. 8) are also consistent with mantle enrichment processes in the Hercynian Belt during the Ordovician.

PETROGENESIS OF PARENTAL CRUST-DERIVED MAGMAS

The selected granitoids, representative of the parental crust-derived magmas in the various sectors of the SCB, belong to the calc-alkaline association (Fig. 2). Their geochemical characteristics are consistent with collision-related granitoids (Fig. 9). Ocean ridge granite-normalized diagrams (Fig. 9) indicate fairly homogeneous elemental enrichment factors of crust-derived magmas along the north–south transverse of the Batholith (~500 km, Fig. 1). The homogeneous composition of granitoids may suggest an origin by partial melting of relatively similar crust. The only exception is the post-tectonic leucogranites, which exhibit, on average, higher Th and lower Ba (and Sr, not shown) enrichment factors than late-tectonic granitoids (Fig. 9). Differences in SiO_2 content (Table 4) suggest, however, that the post-tectonic leucogranites were produced by lower degrees of partial melting than the late-tectonic granitoids (e.g. Poli *et al.*, 1989), and this fact can provide an explanation for differences in Th, Ba and Sr.

In the Rb vs Y+Nb discrimination diagram for the tectonic interpretation of granitoids (Fig. 10), the selected crust-derived magmas plot in the field of volcanic arc granitoids (VAG). On the basis of arguments presented by Pearce *et al.* (1984), post-collisional granitoids can plot in either VAG or syn-collisional granitoid fields, depending on their origin from igneous or sedimentary crustal sources, respectively. Thus, granite magmas from the SCB are likely to derive mainly from igneous and not sedimentary crustal sources as suggested by Cocherie (1984), Rossi & Cocherie (1991) and Cocherie *et al.* (1994). Moreover, experimental petrology data provide evidence for strong peraluminous characteristics of melts produced by melting of sedimentary material (e.g. Montel & Vielzeuf, 1991), whereas the Sardinia–Corsica granitoids have geochemical and petrographic characteristics typical of I-type granitoids (e.g. Bralia *et al.*, 1982; Poli *et al.*, 1989; Poli & Tommasini, 1991*a*; Tommasini, 1993). This conclusion is consistent with that of Poli *et al.* (1989), who suggested, on the basis of trace element modelling, that fluid-absent partial melting processes of igneous crustal sources broadly andesitic in composition could account for the genesis of granite magmas in the SCB.

According to the so-called andesite model (Taylor & McLennan, 1985), addition of new material to the continental crust mainly occurs through lateral and vertical accretion of mantle-derived magmas at active continental margins. Thus, it is possible to envisage a two-stage process for the origin of the parental granite magmas of the SCB: (1) underplating of mantle-derived magmas with formation of large-scale homogeneous crustal sources, basic–intermediate in composition; (2) production of granite magmas through partial melting of the underplated material.

Geochemical data on the nature of the lower crust in the SCB are virtually absent. Major element and REE analysis of one mafic granulite facies xenolith in Plio–Pleistocene alkali basalts from Sardinia has been reported by Rutter (1987). This sample, however, cannot be considered representative of the composition of the lower crust in the SCB. A rough estimate of the composition of the lower crust in the SCB can be inferred from P-wave velocities of seismic profiles of the European Geotraverse (6·6–7·0 km/s from 20 to 30–35 km depth; Ansorge *et al.*, 1992), which support a broadly basic–intermediate igneous composition.

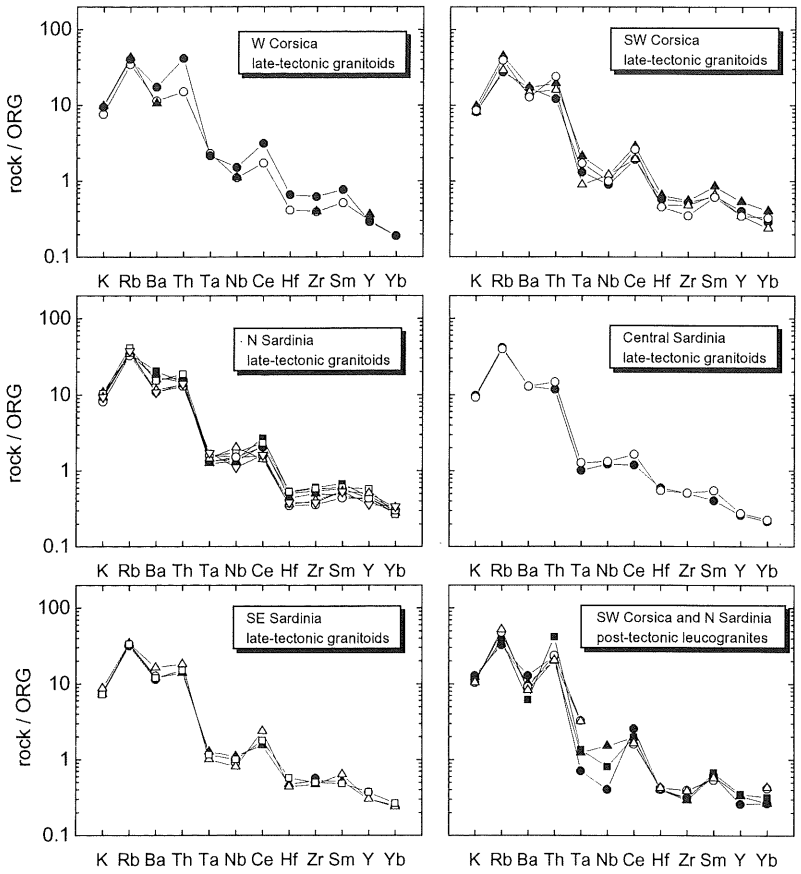

Fig. 9. Ocean ridge granite-normalized diagrams (Pearce *et al.*, 1984) of the selected granitoids from the Sardinia–Corsica Batholith.

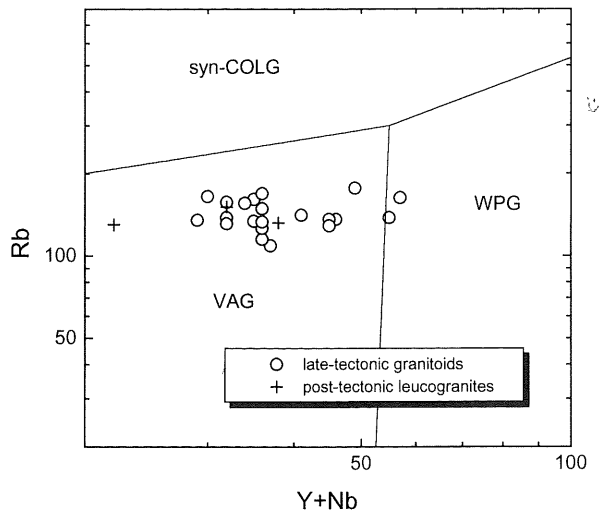

Fig. 10. Rb vs Y + Nb tectonic discrimination diagram (Pearce *et al.*, 1984) of the selected granitoids from the Sardinia–Corsica Batholith. VAG, volcanic arc granitoids; syn-COLG, syn-collisional granitoids; WPG, within-plate granitoids.

Sr and Nd isotope constraints on the formation of the igneous crustal sources

The Sr and Nd isotope compositions of the selected granitoids can place further constraints on the nature of their crustal sources, and provide estimates on the timing of formation. Figure 11 shows $^{87}Sr/^{86}Sr$ and $^{143}Nd/^{144}Nd$ values at 300 Ma for the selected granitoids along with fields of post-tectonic leucogranites (Cocherie, 1984; Beccaluva *et al.*, 1985), and Hercynian I-type granitoids from the French Massif Central (Downes & Duthou, 1988; Pin & Duthou, 1990). Variations in Sr and Nd isotopes from 450 to 300 Ma have been calculated for different crustal components (Fig. 11): (1) orthogneisses, augengneisses and migmatites from the SCB (Beccaluva *et al.*, 1985); (2) orthogneisses, paragneisses and lower-crust metasediments from the French Massif Central (Downes & Duthou, 1988; Downes *et al.*, 1990; Turpin *et al.*, 1990); (3) lower-crust metasediments

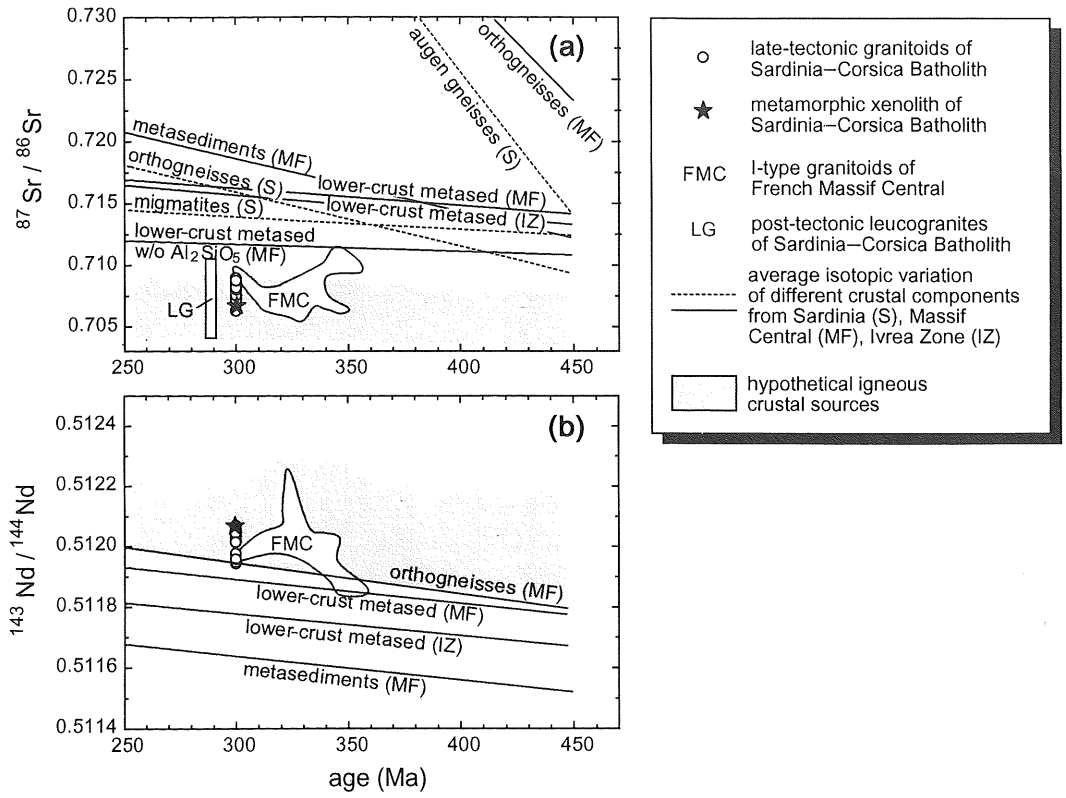

Fig. 11. Variations in $^{87}Sr/^{86}Sr$ (a) and $^{143}Nd/^{144}Nd$ (b) of the hypothetical igneous crustal sources of the selected granitoids from the Sardinia–Corsica Batholith in a time span of 150 Ma (from 450 to 300 Ma). Average isotopic variations of crustal material of Sardinia, Massif Central and Ivrea Zone are from Beccaluva *et al.* (1985), Downes & Duthou (1988), Downes *et al.* (1990), Turpin *et al.* (1990) and Voshage *et al.* (1990). Trace element ratios and isotopic composition of igneous crustal sources at 450 Ma (see text): Rb/Sr = 0·05–0·12, Sm/Nd = 0·20–0·23, $^{87}Sr/^{86}Sr$ = 0·7037–0·7084, $^{143}Nd/^{144}Nd$ = 0·51224–0·51182.

from the Ivrea Zone (Voshage *et al.*, 1990). Average isotopic variations of these crustal components (Fig. 11) provide evidence for negligible contribution of sedimentary and acid igneous material to the genesis of the selected granitoids.

The Sr and Nd isotope compositions of the selected granitoids demand a relatively young juvenile addition to the crust (Fig. 11). In Sardinia, an active continental margin setting was proposed for the earlier Ordovician igneous activity (e.g. Memmi *et al.*, 1983; Carmignani *et al.*, 1992). Thus, extensive underplating of mantle-derived magmas could have occurred in the SCB during the Ordovician, forming middle–lower-crust levels and supplying heat to initiate crustal anatexis (e.g. Huppert & Sparks, 1988). Isotopic data on the Ordovician magmas are limited to Sr isotopes for orthogneisses and augengneisses (Beccaluva *et al.*, 1985). No isotopic data are available for the basic–intermediate calc-alkaline volcanic rocks that can be supposed to be equivalent in composition to the underplated magmas.

Estimates of the Rb/Sr and Sm/Nd values of the hypothetical igneous sources formed during the Ordovician by underplating of mantle-derived magmas can be taken from the andesite bulk crust composition (Taylor & McLennan, 1985), and from average andesite and basaltic andesite compositions of the Andean Cordillera (Wilson, 1989). Preliminary geochemical data on the Ordovician basic–intermediate calc-alkaline volcanic rocks (Poli *et al.*, 1995) are consistent with the assumed values. Sr and Nd isotopes of the hypothetical igneous sources have been assumed considering they were formed by underplating of magmas derived from subcontinental mantle that experienced an enrichment event in the Ordovician. Thus, the range of Sr and Nd isotope compositions at 450 Ma of the igneous crustal sources (Fig. 11) corresponds to that of the enriched subcontinental mantle for mass fractions of sedimentary material added varying from 0·5 to 5 wt% (Fig. 8). Isotopic variations of such hypothetical igneous crustal sources in the 150 Ma time span overlap significantly with $^{87}Sr/^{86}Sr$ and $^{143}Nd/^{144}Nd$ values observed in the granitoids from the SCB and from the French Massif Central (Fig. 11). The overlap provides support for the formation of the crustal sources in the Ordovician.

The Sr and Nd isotope composition of the meta-

igneous xenolith from South-Western Corsica plots within the range of values of the hypothetical igneous crustal sources at 300 Ma (Fig. 11), and places further constraints on the origin of crustal sources of granitoids in the Ordovician. In summary, geochemical and isotopic arguments suggest that I-type granitoids from the SCB originated through partial melting of relatively homogeneous igneous crustal sources, basic–intermediate in composition (e.g. Poli *et al.*, 1989). Formation of these crustal sources, including probably those of I-type granitoids from the French Massif Central, could have occurred by underplating of mantle-derived magmas during the Ordovician calc-alkaline igneous activity.

This tentative scenario for an Ordovician juvenile addition to the crust is a working hypothesis requiring further studies. It is worth mentioning, however, that the Ordovician underplating is consistent with the calc-alkaline igneous activity that occurred between 545 and 410 Ma in the French Massif Central (e.g. Downes & Duthou, 1988; Downes *et al.*, 1990) and between Arenigian and Caradocian in the SCB (e.g. Carmignani *et al.*, 1986). Moreover, Oberli *et al.* (1994) reported the occurrence of island arc metagabbros in the basement of Central Swiss Alps emplaced at ~470 Ma (single crystal U–Pb dating on zircon).

GEODYNAMIC IMPLICATIONS

Geochemical and isotopic characteristics of parental mantle- and crust-derived magmas from the SCB indicate that:

(1) the mantle sources of basic magmas experienced enrichment in incompatible trace elements through recycling of sedimentary material via subduction zones;

(2) the enrichment could be related to the earlier Ordovician igneous activity that took place in an active continental margin setting (e.g. Memmi *et al.*, 1983; Carmignani *et al.*, 1992);

(3) the main component of the crustal sources of the granite magmas is likely to be an igneous protolith;

(4) the formation of the crustal sources could be related to a major crustal accretion event that occurred during the earlier Ordovician igneous activity by underplating of mantle-derived magmas.

These conclusions, along with available geochronological data of the main Palaeozoic events in Sardinia and Corsica (Table 1), permit the delineation of a geodynamic model for the evolution of the continental lithosphere in this sector of the European Hercynian Belt. Geochemical and isotopic data on Hercynian calc-alkaline magmas suggest a connection between the Ordovician and Hercynian igneous activity. The two magmatic cycles can be placed in a single and wider geodynamic setting consisting of (1) an Ordovician pre-collisional phase, (2) a Devonian collisional phase and (3) a Carboniferous post-collisional phase.

The pre-collisional phase developed during the Ordovician, following Cambro-Ordovician crustal thinning and sea-floor spreading (e.g. Pin, 1990; Carmignani *et al.*, 1992). It has been characterized by subduction of oceanic crust under continental crust and formation of a volcanic arc (Memmi *et al.*, 1983; Carmignani *et al.*, 1992).The downgoing oceanic slab dipped toward the N–NE as suggested by the metamorphic polarity (Fig. 1) and by the S–SW vergence of overthrusting crustal nappes developed during the Hercynian orogeny (e.g. Di Simplicio *et al.*, 1974; Carmignani *et al.*, 1986, 1987, 1992; Franceschelli *et al.*, 1989). A major crustal accretion event took place through underplating of mantle-derived magmas and determined the formation of relatively homogeneous igneous sources in the middle–lower crust of the Sardinia–Corsica basement. Also, underplating of mantle-derived magmas supplied heat to initiate crustal anatexis with formation of volcanic and intrusive acid rocks (i.e. the Ordovician igneous activity). Enrichment in incompatible trace elements in the subcontinental mantle wedge above the subducting oceanic slab occurred through recycling of sedimentary material.

The collisional phase took place after the total consumption of the oceanic plate. The age of the medium-pressure–high-temperature metamorphic peak at 350 Ma (Table 1) places constraints for Devonian commencement of the collisional phase on the basis of theoretical models on P–T–t paths in continental collision settings (e.g. England & Thompson, 1984; Spear, 1989). The collision is supported by Early Carboniferous flysch deposits outcropping in Southern Sardinia (Barca, 1991; Carmignani *et al.*, 1992). They are terrigenous synorogenic deposits that interrupt the sedimentation in the Devonian–Early Carboniferous carbonate platforms. Continental collision caused crustal thickening with overthrusting of crustal blocks along with Barrovian-type metamorphic events that recorded a clockwise P–T–t path (e.g. Franceschelli *et al.*, 1989; Carmignani *et al.*, 1992). The time span between continental collision and the beginning of the Hercynian igneous activity (350–330 Ma, Table 1) is estimated at 35–55 Ma, and is consistent with the time required to achieve crustal anatexis in continental thickened orogenic belts (e.g. England & Thompson, 1984; Peacock, 1989).

The post-collisional phase developed during the Carboniferous, and was characterized by basement uplift and low-pressure–high-temperature metamorphic events (Table 1) owing to isostatic and thermal readjustments following crustal thickening (Franceschelli *et al.*, 1989; Carmignani *et al.*, 1992). Isostatic and thermal readjustments determined the attainment of conditions for extensive partial melting processes in the pile of overthrusted crustal blocks and subcontinental mantle (e.g. England & Thompson, 1984) with the production of large quantities of granites and minor gabbros (i.e. the Hercynian igneous activity). Granite magmas were emplaced in both forced (i.e. late-tectonic granitoids) and permissive (i.e. post-tectonic leucogranites) regimes. Partial melting involved different source components piled up during the collisional phase, namely, in order of amount of magma generated and referring to the pre-collisional structure of continental lithosphere underneath Sardinia and Corsica: (1) middle–lower-crust levels formed during the Ordovician crustal accretion event through underplating of mantle-derived magmas; (2) upper-crust levels mainly composed by sedimentary and acid igneous material; (3) subcontinental mantle enriched through recycling of crustal material.

The middle–lower-crust levels were the main source component of both late-tectonic granitoids and post-tectonic leucogranites (Poli *et al.*, 1989; Tommasini, 1993). The upper-crust levels produced peraluminous granitoids whose geochemical characteristics and genetic relationships have been dealt with elsewhere (e.g. Macera *et al.*, 1989; Poli *et al.*, 1989; Di Vincenzo & Ghezzo, 1992). The subcontinental mantle formed calc-alkaline basic magmas (Tommasini, 1993). Granite and basic magmas along with their interaction products (e.g. Cocherie, 1984; Poli *et al.*, 1989; Poli & Tommasini, 1991*b*; Rossi & Cocherie, 1991; Zorpi *et al.*, 1991; Tommasini, 1993) created the main frame of the SCB (Fig.1) in a time span of ~30 Ma (Table 1).

Comparison with Palaeozoic evolution of Western Europe

The reliability of the Palaeozoic geodynamic evolution of Sardinia and Corsica inferred on the basis of geochemical and isotopic characteristics of Hercynian mantle- and crust-derived magmas can be assessed by comparison with geodynamic models developed for other sectors of Western Europe and based on the interpretation of geological, geochronological and palaeomagnetic data (e.g. Lefort, 1979; Lefort & Van der Voo, 1981; Matte, 1986; Ziegler, 1986; Burg *et al.*, 1987; Pin, 1990). In the geodynamic model of Ziegler (1986), a complex mosaic of a number of Gondwana-derived microcratons were accreted to the southern margins of Laurasia from Ordovician to Early Carboniferous. The evolution of Europe was dominated by continued northward subduction of the proto-Tethys plate at an arc–trench system. The collision of Gondwana with Laurasia marked the onset of the Hercynian orogeny. Burg *et al.* (1987) suggested a continuous evolution of the Ibero-Aquitanian and Armorican continental plates from Ordovician to Carboniferous. The relevant features of their model were (fig. 9 of Burg *et al.*, 1987): (1) the N–NE-dipping subduction of the South Armorican (Paris & Robardet, 1990) or Massif Central (Matte, 1986) oceanic plate under the Armorican plate in Late Ordovician; (2) the collision between the Ibero-Aquitanian and Armorican continental plates in Late Silurian–Early Devonian.

A widespread subduction-related geodynamic setting in Western Europe during the Ordovician is supported by a high-pressure granulite–eclogite facies event which occurred between 450 and 390 Ma (e.g. Pin & Vielzeuf, 1983; Vielzeuf & Pin, 1989; Pin, 1990), recorded by several ophiolitic complexes and crustal rocks outcropping in the suture zone that can be followed along a narrow belt from the Iberian Peninsula to Brittany and the Massif Central (e.g. Lefort, 1979; Burg *et al.*, 1987; Pin, 1990). Moreover, calc-alkaline igneous activity occurred between 545 and 410 Ma in the French Massif Central (e.g. Downes & Duthou, 1988; Downes *et al.*, 1990). Arc-related volcanic rocks were found in the Southern Armorican Massif (Thiéblemont & Cabanis, 1986). Island arc metagabbros were emplaced at ~470 Ma in the Central Swiss Alps (Oberli *et al.*, 1994).

The palaeomagnetic restoration of the Late Palaeozoic position of Sardinia and Corsica close to Southern France (Auzende *et al.*, 1973; Westphal *et al.*, 1976; Edel *et al.*, 1981) suggests that the evolution of the Sardinia–Corsica continental block could be referred to that of the southern edge of the Armorican plate. Thus, the model proposed in the present paper is consistent with that suggested by Burg *et al.* (1987). The geochemical and isotopic similarities of Hercynian calc-alkaline magmas from the SCB and the French Massif Central provide further evidence for a common evolution of the continental lithosphere of Southern France and Sardinia and Corsica during the Palaeozoic.

The proposed geodynamic reconstruction is not meant to be exhaustive, for a number of aspects have not been dealt with, namely: (1) the Silurian within-plate magmatism (e.g. Ricci & Sabatini, 1978); (2) the sources of the Mg–K or shoshonitic association

outcropping in North-Western Corsica (Fig. 1); (3) the timing of the high-pressure granulite–eclogite facies event recorded by some metamorphic rocks outcropping in Northern Sardinia and South-Eastern Corsica (e.g. Miller *et al.*, 1976; Ghezzo *et al.*, 1979; Palagi *et al.*, 1985; Libourel & Vielzeuf, 1988). The geodynamic reconstruction aims to serve as a working model for future research on the Palaeozoic basement of Sardinia and Corsica. In particular, it is worth establishing whether other magmatic and metamorphic events can be placed in the geodynamic model, to yield a complete scenario of lithosphere evolution in this sector of the European Hercynian Belt during the Palaeozoic. A detailed study is also in progress on the geochemical characteristics of the basic–intermediate volcanic rocks of the Ordovician igneous activity (e.g. Poli *et al.*, 1995).

ACKNOWLEDGEMENTS

We thank Gareth R. Davies, Angelo Peccerillo and Sandro Conticelli for comments on an earlier version of the manuscript. We are also grateful to Christian Pin and Hilary Downes for helpful suggestions and criticism in reviewing the manuscript. S. T. wishes to express his special thanks to Der-Chuen Lee and Matthias Ohr for their skilful assistance during isotope analyses while at the University of Michigan. Research was supported by Italian MURST Grants 40% and 60% to G. P. Isotopic studies were also supported by NSF Grants EAR 90-04133 and 92-05435 to A. N. H.

REFERENCES

Ansorge, J., Blundell, D. & Mueller, S., 1992. Europe's lithosphere—seismic structure. In: Blundell, D., Freeman, R. & Mueller, S. (eds) *A Continent Revealed—The European Geotraverse*. Cambridge: Cambridge University Press, pp. 33–69.

Auzende, J. M., Bonnin, J. & Olivet, J. L., 1973. Hypotheses on the origin of the western Mediterranean basin. *Journal of the Geological Society of London* **129,** 607–620.

Barca, S., 1991. Phénomènes de resédimentation et flysch hercynien à faciès Culm dans le synclinal du Sarrabus (SE de la Sardaigne, Italie). *Comptes Rendus Hebdomadaires de l'Académie des Sciences* **313,** 1051–1057.

Beccaluva, L., Civetta, L., Macciotta, G. & Ricci, C. A., 1985. Geochronology in Sardinia: results and problems. *Rendiconti della Società Italiana di Mineralogia e Petrologia* **40,** 57–72.

Bonin, B., 1980. Les complexes alcaliens acides anorogéniques: l'exemple de la Corse. Thèse d'Etat, University of Paris VI, 779 pp.

Bonin, B., 1988. From orogenic to anorogenic environments: evidence from associated magmatic episodes. *Schweizerische Mineralogische und Petrographische Mitteilungen* **68,** 301–311.

Bralia, A., Ghezzo, C., Guasparri, G. & Sabatini, G., 1982. Aspetti genetici del batolite ercinico sardo. *Rendiconti della Società Italiana di Mineralogia e Petrologia* **38,** 701–764.

Brown, L., Klein, J., Middleton, R., Sacks, I. S. & Tera, F., 1982. ^{10}Be in island-arc volcanoes and implications for subduction. *Nature* **299,** 718–720.

Burg, J. P., Bale, P., Brun, J. P. & Girardeau, J., 1987. Stretching lineation and transport direction in the Ibero-Armorican arc during the Siluro-Devonian collision. *Geodinamica Acta* **1,** 71–87.

Carmignani, L., Barca, S., Cappelli, B., Di Pisa, A., Gattiglio, M., Oggiano, G. & Pertusati, P. C., 1992. A tentative geodynamic model for the Hercynian basement of Sardinia. In: Carmignani, L. & Sassi, F. P. (eds) *Contributions to the Geology of Italy. IGCP 276, Newsletter* **5,** 61–82.

Carmignani, L., Cherchi, A. & Ricci, C. A., 1987. Basement structure and Mesozoic–Cenozoic evolution of Sardinia. In: Boriani, A., Bonafede, M., Piccardo, G. B. & Vai, G. B. (eds) *The Lithosphere in Italy*. Roma: Accademia Nazionale dei Lincei, pp. 63–92.

Carmignani, L., Cocozza, T., Ghezzo, C., Pertusati, P. C. & Ricci, C. A., 1986. Outlines of the Hercynian basement of Sardinia. In: Carmignani, L., Cocozza, T., Ghezzo, C., Pertusati, P. C. & Ricci, C. A. (eds) *Guide-book to the Excursion on the Palaeozoic Basement of Sardinia. IGCP 5, Newsletter*, Special Issue, 11–21.

Cocherie, A., 1984. Interaction manteau–croûte: son rôle dans la genèse d'associations plutoniques calco-alcalines, contraintes géochimiques (élément en traces et isotopes du strontium et de l'oxygène). Thèse d'Etat, University of Rennes I, 245 pp.

Cocherie, A., Rossi, Ph., Fouillac, A. M. & Vidal, Ph., 1994. Crust and mantle contributions to granite genesis—an example from the Variscan batholith of Corsica, France, studied by trace element and Nd–Sr–O isotope systematics. *Chemical Geology* **115,** 173–211.

Di Simplicio, P., Ferrara, G., Ghezzo, C., Guasparri, G., Pellizzer, R., Ricci, C. A., Rita, F. & Sabatini, G., 1974. Il metamorfismo e il magmatismo paleozoico della Sardegna. *Rendiconti della Società Italiana di Mineralogia e Petrologia* **30,** 979–1068.

Di Vincenzo, G. & Ghezzo, C., 1992. Peraluminous Hercynian granitoids in Sardinia, Corsica and Provence: a preliminary note. In: Carmignani, L. & Sassi, F.P. (eds) *Contributions to the Geology of Italy. IGCP 276, Newsletter* **5,** 469–472.

Downes, H. & Dupuy, C., 1987. Textural, isotopic and REE variations in spinel peridotite xenoliths, Massif Central, France. *Earth and Planetary Science Letters* **82,** 121–135.

Downes, H., Dupuy, C. & Leyreloup, A. F., 1990. Crustal evolution of the Hercynian belt of Western Europe: evidence from lower-crustal granulitic xenoliths (French Massif Central). *Chemical Geology* **83,** 209–231.

Downes, H. & Duthou, J. L., 1988. Isotopic and trace element arguments for the lower-crustal origin of Hercynian granitoids and pre-Hercynian orthogneisses, Massif Central (France). *Chemical Geology* **68,** 291–308.

Dunai, T. J. & Baur, H., 1995. Helium-, neon- and argon-systematics of the European subcontinental mantle: implications for its geochemical evolution. *Geochimica et Cosmochimica Acta* **59,** 2767–2783.

Edel, J. B., Montigny, R. & Thuizat, R., 1981. Late Paleozoic rotations of Corsica and Sardinia: new evidence from paleomagnetic and K–Ar studies. *Tectonophysics* **79,** 201–223.

England, P. C. & Thompson, A. B., 1984. Pressure–temperature–time paths of regional metamorphism I. Heat transfer during the evolution of regions of thickened continental crust. *Journal of Petrology* **25,** 894–928.

Faure, G., 1986. *Principles of Isotope Geology*. New York: John Wiley, 589 pp.

Franceschelli, M., Memmi, I., Pannuti, F. & Ricci, C. A., 1989. Diachronous metamorphic equilibria in the Hercynian basement of Northern Sardinia, Italy. In: Daly, J. F., Cliff, R. A. & Yardley, W. D. (eds) *Evolution of Metamorphic Belts. Geological Society Special Publication* **43,** 371–375.

Franzini, M. & Leoni, L., 1972. A full matrix correction in X-ray fluorescence analysis of rock samples. *Atti della Società Toscana di Scienze Naturali di Pisa Memorie* **79**(A), 7–22.

Frost, T. P. & Lindsay, J. R., 1988. Magmix: a basic program to calculate viscosities of interacting magmas of differing composition, temperature, and water content. *Computers and Geosciences* **14,** 213–228.

Frost, T. P. & Mahood, G. A., 1987. Field, chemical and physical constraints on mafic–felsic magma interaction in the Lamark Granodiorite, Sierra Nevada, California. *Geological Society of America Bulletin* **99,** 272–291.

Ghezzo, C., Memmi, I. & Ricci, C. A., 1979. Un evento granulitico nel basamento metamorfico della Sardegna nord-orientale. *Memorie della Società Geologica Italiana* **20,** 23–38.

Gill, J. B., 1981. *Orogenic Andesites and Plate Tectonics*. Berlin: Springer-Verlag, 390 pp.

Green, D. H., 1973. Experimental melting studies on a model upper mantle composition at high pressure under water-saturated and water-undersaturated conditions. *Earth and Planetary Science Letters* **19,** 37–53.

Green, D. H., 1976. Experimental testing of equilibrium partial melting of peridotite under water-saturated, high pressure conditions. *Canadian Mineralogist* **14,** 255–268.

Halliday, A. N., Davidson, J. P., Holden, P., DeWolf, C., Lee, D. C. & Fitton, G., 1990. Trace element fractionation in plumes and the origin of HIMU mantle beneath the Cameroon line. *Nature* **347,** 523–528.

Halliday, A. N., Mahood, G. A., Holden, P., Metz, J. M., Dempster, T. J. & Davidson, J. P., 1989. Evidence for long residence times of rhyolitic magma in the Long Valley magmatic system: the isotopic record in precaldera lavas of Glass Mountain. *Earth and Planetary Science Letters* **94,** 274–290.

Henderson, P., 1986. *Inorganic Geochemistry*. Oxford: Pergamon Press, 353 pp.

Hildreth, E. W. & Moorbath, S., 1988. Crustal contribution to arc magmatism in the Andes of Central Chile. *Contributions to Mineralogy and Petrology* **98,** 455–489.

Hofmann, A. W., Jochum, K. P., Saufert, M. & White, W. M., 1986. Nb and Pb in oceanic basalts: new constraints on mantle evolution. *Earth and Planetary Science Letters* **79,** 33–45.

Huppert, H. E. & Sparks, R. S. J., 1988. The generation of granitic magmas by intrusion of basalt into continental crust. *Journal of Petrology* **29,** 599–624.

Jagoutz, E., Palme, H., Baddenhausen, H., Blum, K., Cendales, M., Dreibus, G., Spettel, B., Lorenz, V. & Wanke, H., 1979. The abundances of major, minor and trace elements in the earth's mantle as derived from primitive ultramafic nodules. *Proceedings of the 10th Lunar Planetary Science Conference. Geochimica et Cosmochimica Acta* Supplement, 2031–2050.

Jochum, K. P., McDonough, W. F., Palme, H. & Spettel, B., 1989. Compositional constraints on the continental lithospheric mantle from trace elements in spinel peridotite xenoliths. *Nature* **340,** 548–550.

Johnston, A. D. & Wyllie, P. J., 1988. Interaction of granitic and basic magmas: experimental observations on contamination processes at 10 kbar with H_2O. *Contributions to Mineralogy and Petrology* **98,** 352–362.

Kaye, M. J., 1965. X-ray fluorescence determinations of several trace elements in some standard geochemical samples. *Geochimica et Cosmochimica Acta* **29,** 139–142.

Lefort, J. P., 1979. Iberian–Armorican arc and Hercynian orogeny in western Europe. *Geology* **7,** 384–388.

Lefort, J. P. & van der Voo, R., 1981. A kinematic model for the collision and complete suturing between Gondwanaland and Laurussia in the Carboniferous. *Journal of Geology* **89,** 537–550.

Libourel, G. & Vielzeuf, D., 1988. Isobaric cooling at high pressure: example of Corsican high pressure granulites. *Granulite Conference*, Clermont Ferrand, France. *Terra Cognita* **8,** 268 (abstract).

Macera, P., Conticelli, S., Del Moro, A., Di Pisa, A., Oggiano, G. & Squadrone, A., 1989. Geochemistry and Rb/Sr age of syntectonic peraluminous granites of Western Gallura, Northern Sardinia: contraints on their genesis. *Periodico di Mineralogia* **58,** 25–43.

Matte, P., 1986. La chaîne varisque parmi les chaînes paléozoiques péri-atlantiques, modèle d'évolution et position des grands blocs continentaux au Permo-Carbonifère. *Bulletin de la Société Géologique de France* **8,** 9–24.

McCulloch, M. T. & Perfit, M. R., 1981. $^{143}Nd/^{144}Nd$, $^{87}Sr/^{86}Sr$ and trace element constraints on the petrogenesis of Aleutian island arc magmas. *Earth and Planetary Science Letters* **56,** 167.

McDonough, W. F., 1990. Constraints on the composition of the continental lithospheric mantle. *Earth and Planetary Science Letters* **101,** 1–18.

Memmi, I., Barca, S., Carmignani, L., Cocozza, T., Elter, F., Franceschelli, M., Gattiglio, M., Ghezzo, C., Minzoni, N., Naud, G., Pertusati, P. C. & Ricci, C. A., 1983. Further geochemical data on the pre-Hercynian igneous activities of Sardinia and on their geodynamic significance. *IGCP 5 Newsletter* **5,** 87–93.

Ménot, R. P. & Orsini, J. B., 1990. Evolution du socle anté-stéphanien de Corse: évènements magmatiques et métamorphiques. *Schweizerische Mineralogische und Petrographische Mitteilungen* **70,** 35–53.

Miller, L., Sassi, F. P. & Armari, G., 1976. On the occurrence of altered eclogite rocks in north-eastern Sardinia and their implications. *Neues Jahrbuch für Geologie und Paläontologie, Monatshefte* **11,** 683–689.

Miyashiro, A., 1978. Nature of alkalic volcanic rock series. *Contributions to Mineralogy and Petrology* **66,** 91–104.

Montel, J. M. & Vielzeuf, D., 1991. Experimental partial melting of a natural quartz-rich greywacke (II): phase compositions and *P–T–F* (melt fraction) relationships. *Terra* **3,** 29–30 (abstract).

Oberli, F., Meier, M. & Biino, G. G., 1994. High-resolution single crystal U–Pb dating of Ordovician eclogites—tracers for the early evolution of a Central Swiss alpine terrane. In: Lanphere, M. A., Dalrymple, G. B. & Turrin, B. D. (eds) *ICOG 8, US Geological Survey Circular* **1107,** 237 (abstract).

Orsini, J. B., 1980. Le Batholite Corso–Sarde: anatomie d'un batholite hercynien. Thèse d'Etat, University of Aix–Marseille III, 390 pp.

Palagi, P., Laporte, D., Lardeaux, J.M., Ménot, R. P. & Orsini, J.B., 1985. Identification d'un complexe leptyno-amphibolique au sein des 'gneiss de Belgodere' (Corse occidentale). *Comptes Rendus Hebdomadaires de l'Académie des Sciences* **301,** 1047–1052.

Paris, F. & Robardet, M., 1990. Early Paleozoic palaeobiogeography of the Variscan regions. *Tectonophysics* **177,** 193–213.

Peacock, S. M., 1989. Thermal modeling of metamorphic pressure–temperature–time paths: a forward approach. In: Crawford, M. L. & Padovani, E. (eds) *Metamorphic Pressure–*

Temperature–Time Paths. Short Course in Geology, 7. Washington, DC: American Geophysical Union, pp. 57–102.

Pearce, J. A., 1982. Trace element characteristics of lavas from destructive plate boundaries. In: Thorpe, R. S. (ed.) *Andesites: Orogenic Andesites and Related Rocks.* New York: John Wiley, pp. 525–548.

Pearce, J. A. & Cann, J. R., 1973. Tectonic setting of basic volcanic rocks determined using trace element analysis. *Earth and Planetary Science Letters* **19,** 290–300.

Pearce, J. A., Harris, N. B. & Tindle, A. G., 1984. Trace element discrimination diagrams for the tectonic interpretation of granitic rocks. *Journal of Petrology* **25,** 956–983.

Peccerillo, A. & Taylor, S. R., 1976. Geochemistry of Eocene calc-alkaline volcanic from the Kastamonu area, northern Turkey. *Contributions to Mineralogy and Petrology* **58,** 63–81.

Perfit, M. R., Gust, D. A., Bence, A. E., Arculus, R. J. & Taylor, S. R., 1980. Chemical characteristics of island arc basalts: implications for mantle sources. *Chemical Geology* **30,** 227–256.

Pin, C., 1990. Variscan oceans: ages, origins and geodynamic implications inferred from geochemical and radiometric data. *Tectonophysics* **177,** 215–227.

Pin, C. & Duthou, J. L., 1990. Sources of Hercynian granitoids from the French Massif Central: inferences from Nd isotopes and consequences for crustal evolution. *Chemical Geology* **83,** 281–296.

Pin, C. & Vielzeuf, D, 1983. Granulites and related rocks in Variscan median Europe: a dualistic interpretation. *Tectonophysics* **93,** 47–74.

Poli, G., Ghezzo, C. & Conticelli, S., 1989. Geochemistry of granitic rocks from the Hercynian Sardinia–Corsica Batholith: implication for magma genesis. *Lithos* **23,** 247–266.

Poli, G., Manetti, P., Peccerillo, A. & Cecchi, A., 1977. Determinazione di alcuni elementi del gruppo delle terre rare in rocce silicatiche per attivazione neutronica. *Rendiconti della Società Italiana di Mineralogia e Petrologia* **33,** 755–763.

Poli, G., Martelli, R., Manetti, P. & Tommasini, S., 1995. Petrology of the Ordovician igneous activity in the Sardinia Corsica Batholith. *EUG 8,* Strasbourg, France, April 1995. *Terra* **7,** 299 (abstract).

Poli, G. & Tommasini, S., 1991*a*. A geochemical approach to the evolution of granitic plutons: a case study, the acid intrusions of Punta Falcone (northern Sardinia, Italy). *Chemical Geology* **92,** 87–105.

Poli, G. & Tommasini, S., 1991*b*. Model for the origin and significance of microgranular enclaves in calc-alkaline granitoids. *Journal of Petrology* **32,** 657–666.

Ricci, C. A. & Sabatini, G., 1978. Petrogenetic affinity and geodynamic significance of metabasic rocks from Sardinia, Corsica and Provence. *Neues Jahrbuch für Geologie und Paläontologie, Monatshefte* **1,** 23–38.

Rossi, P., 1986. Organisation et genèse d'un grand batholite orogénique: le Batholite calco-alcalin de la Corse. Thèse d'Etat, University of Toulouse, 292 pp.

Rossi, P. & Cocherie, A., 1991. Genesis of a Variscan batholith: field, petrological and mineralogical evidence from the Corsica–Sardinia Batholith. *Tectonophysics* **195,** 319–346.

Rutter, M. J., 1987. The nature of the lithosphere beneath the Sardinian continental block: mantle and deep crustal inclusions in mafic alkaline lavas. *Lithos* **20,** 225–234.

Shaw, A., Downes, H. & Thirlwall, M. F., 1993. The quartz-diorites of Limousin: elemental and isotopic evidence for Devono-Carboniferous subduction in the Hercynian belt of the French Massif Central. *Chemical Geology* **107,** 1–18.

Spear, F. S., 1989. Petrologic determination of metamorphic pressure–temperature–time paths. In: Crawford, M. L. & Padovani, E. (eds) *Metamorphic Pressure–Temperature–Time Paths. Short Course in Geology, 7.* Washington, DC: American Geophysical Union, pp. 1–55.

Sun, S. S. & McDonough, W. F., 1989. Chemical and isotopic systematics of oceanic basalts: implications for mantle composition and processes. In: Saunders, A. D. & Norry, M. J. (eds) *Magmatism in the Ocean Basins. Geological Society Special Publication* **42,** 313–345.

Taylor, S. R. & McLennan, S. M., 1985. *The Continental Crust: its Composition and Evolution.* Oxford: Blackwell Scientific, 312 pp.

Thiéblemont, D. & Cabanis, B., 1986. Découverte d'une association de volcanites d'arc et de basaltes de type MORB dans la formation pal-volcanique silurienne de la Meilleraie, Vendée, France. *Comptes Rendus Hebdomadaires de l'Académie des Sciences* **302,** 641–646.

Tommasini, S., 1993. Petrologia del magmatismo calcalcalino del Batolite Sardo–Corso: processi genetici ed evolutivi dei magmi in aree di collisione continentale e implicazioni geodinamiche. Ph.D. Thesis, University of Perugia, 326 pp.

Tommasini, S. & Poli, G., 1992. Petrology of the late-Carboniferous Punta Falcone gabbroic complex, northern Sardinia, Italy. *Contributions to Mineralogy and Petrology* **110,** 16–32.

Turpin, L., Cuney, M., Friedrich, M., Bouchez, J. L. & Aubertin, M., 1990. Meta-igneous origin of Hercynian peraluminous granites in N.W. French Massif Central: implications for crustal history reconstructions. *Contributions to Mineralogy and Petrology* **104,** 163–172.

Turpin, L., Velde, D. & Pinte, G., 1988. Geochemical comparison between minettes and kersantites from the Western European Hercynian orogen: trace element and Pb–Sr–Nd isotope constraints on their origin. *Earth and Planetary Science Letters* **87,** 73–86.

Vellutini, P., 1977. Le magmatisme permien de la Corse du nord-ouest. Thèse d'Etat, University of Aix–Marseille III, 317 pp.

Vezat, R., 1986. Le batholite calco-alcalin de Corse, les formations métamorphiques calédono-varisques de Zicavo, la mise en place du batholite calco-alcalin. Thèse d'Etat, University Paul Sabatier, Toulouse, 364 pp.

Vielzeuf, D. & Pin, C., 1989. Geodynamic implications of granulitic rocks in the Hercynian belt. In: Daly, J. F., Cliff, R. A. & Yardley, W. D. (eds) *Evolution of Metamorphic Belts. Geological Society Special Publication* **43,** 343–348.

Voshage, H., Hofmann, A. W., Mazzucchelli, M., Rivalenti, G., Sinigoi, S., Raczek, I. & Demarchi, G., 1990. Isotopic evidence from the Ivrea Zone for a hybrid lower crust formed by magmatic underplating. *Nature* **347,** 731–736.

Weaver, B. L. & Tarney, J., 1981. Lewisian geochemistry and Archean crustal development models. *Earth and Planetary Science Letters* **55,** 171–180.

Westphal, M., Orsini, J. B. & Vellutini, P., 1976. Le micro-continent corso-sarde, sa position initiale: données paléomagnétiques et raccords géologiques. *Tectonophysics* **30,** 141–157.

White, W. M. & Dupre, B., 1986. Sediment subduction and magma genesis in the Lesser Antilles: isotopic and trace element constraints. *Journal of Geophysical Research* **91**(B6), 5927–5941.

White, W. M., Dupre, B. & Vidal, P., 1985. Isotope and trace element geochemistry of sediments from the Barbados Ridge–Demerara Plain region, Atlantic Ocean. *Geochimica et Cosmochimica Acta* **49,** 1875–1886.

White, W. M. & Patchett, J., 1984. Hf–Nd–Sr isotopes and incompatible element abundances in island arcs: implication for magma origins and crust–mantle evolution. *Earth and Planetary Science Letters* **67,** 167.

Wilson, M., 1989. *Igneous Petrogenesis*. London: Unwin Hyman, 466 pp.

Winchester, J. A. & Floyd, P. A., 1977. Geochemical discrimination of different magma series and their differentiation products using immobile elements. *Chemical Geology* **20,** 325–343.

Wood, D. A., 1979. A variably veined suboceanic upper mantle. Genetic significance for mid-ocean ridge basalts from geochemical evidence. *Geology* **7,** 499–503.

Ziegler, P. A., 1986. Geodynamic model for the Palaeozoic crustal consolidation of western and central Europe. *Tectonophysics* **126,** 303–328.

Zorpi, M. J., Coulon, C. & Orsini, J. B., 1991. Hybridization between felsic and mafic magmas in calc-alkaline granitoids—a case study in northern Sardinia, Italy. *Chemical Geology* **92,** 45–86.

RECEIVED OCTOBER 25, 1994
REVISED TYPESCRIPT ACCEPTED MARCH 24, 1995

APPENDIX: ANALYTICAL METHODS FOR ISOTOPE ANALYSES

Isotope analyses were performed at the Radiogenic Isotope Geochemistry Laboratory of the University of Michigan. Approximately 30 mg of sample powder was dissolved in pressurized Teflon PFA vials using an $HF–HNO_3$ mixture. After 2–3 days the sample was evaporated to dryness and was then completely soluble in hot 6 N HCl. Duplicate measurements using screw-top, Teflon PFA vials inside Teflon digestion bombs resulted in no significant differences in $^{143}Nd/^{144}Nd$. Roughly 20% of the solution was spiked using mixed ^{87}Rb–^{84}Sr and ^{149}Sm–^{150}Nd spikes. Rb, Sr and REE were separated using 3 ml of AG50W × 8 cation exchange resin, whereas Sm and Nd were separated using a 3 ml column of PTFE coated with HDEHP. The total procedure blanks for Sr and Nd were typically <100 and 30 pg, respectively, at the time of these analyses. Isotopic ratios were measured on two VG Sector thermal ionization mass spectrometers with multiple Faraday collectors. Nd and Sr isotope compositions were measured in multi-dynamic mode, and were normalized to $^{86}Sr/^{88}Sr = 0{\cdot}1194$ and $^{146}Nd/^{144}Nd = 0{\cdot}7219$, respectively. Uncertainty in Rb/Sr and Sm/Nd was $\leqslant 1\%$ and $\leqslant 0{\cdot}2\%$, respectively. The $^{87}Sr/^{86}Sr$ of NIST SRM987 was $0{\cdot}71025 \pm 1$ (2σ, $N = 20$) and the $^{143}Nd/^{144}Nd$ of the La Jolla Nd standard was $0{\cdot}51185 \pm 1$ (2σ, $N = 20$) at the time of data collection. Further analytical details have been reported by Halliday *et al.* (1989, 1990).